Renewable and Sustainable Energy Reviews 40 (2014) 237–259

Contents lists available at ScienceDirect

Renewable and Sustainable Energy Reviews

journal homepage: www.elsevier.com/locate/rser

Preparation, thermal properties and applications of shape-stabilized thermal energy storage materials

Guiyin Fang*, Fang Tang, Lei Cao

School of Physics, Nanjing University, Nanjing 210093, China

ARTICLE INFO

Article history:
Received 29 January 2014
Received in revised form
23 June 2014
Accepted 21 July 2014

Keywords:
Shape-stabilized
Composite phase change material
Microencapsulated phase change material
Thermal properties
Thermal energy storage

ABSTRACT

Phase change materials (PCMs) have received attention for various applications in solar heating systems, building energy conservation and air-conditioning systems. However, they need encapsulation in order to prevent leakage of the melted PCM during the phase change process. Now, these problems can be solved by using shape-stabilized PCMs. These shape-stabilized PCMs can be prepared by integrating the PCMs into the supporting material and microencapsulating the PCMs into the shell. This paper presents a review on preparation, thermal properties and applications of shape-stabilized thermal energy storage materials. The thermal properties of the composite phase change material and microencapsulated phase change material are analyzed and discussed. The applications of shape-stabilized thermal energy storage materials are summarized.

© 2014 Elsevier Ltd. All rights reserved.

Contents

1. Introduction . . . 238
2. Preparation and thermal properties of composite phase change materials . . . 238
   2.1. Composite phase change materials with organic supporting material . . . 238
   2.2. Composite phase change materials with inorganic supporting material . . . 242
   2.3. Comparison of composite phase change materials with organic and inorganic supporting material . . . 244
3. Preparation and thermal properties of microencapsulated phase change materials . . . 244
   3.1. Microencapsulated phase change materials with organic shell . . . 245
   3.2. Microencapsulated phase change materials with inorganic shell . . . 247
   3.3. Comparison of microencapsulated phase change materials with organic and inorganic shell . . . 248
4. Various encapsulation techniques of the microencapsulated phase change materials . . . 249
   4.1. In situ polymerization . . . 249
   4.2. Interfacial polymerization . . . 250
   4.3. Suspension polymerization . . . 250
   4.4. Sol–gel polymerization . . . 250
   4.5. Complex coacervation . . . 251
   4.6. Spray drying . . . 251
   4.7. Comparison of various encapsulation techniques . . . 252
5. Applications of shape-stabilized thermal energy storage materials . . . 252
   5.1. Applications of composite phase change materials . . . 252
   5.2. Applications of microencapsulated phase change materials . . . 254
   5.3. Applications of shape-stabilized phase change materials in engineering project . . . 255
      5.3.1. Applications of composite phase change materials in engineering project . . . 255

* Corresponding author. Tel.: +86 25 51788228; fax: +86 25 83593707.
E-mail address: gyfang@nju.edu.cn (G. Fang).

http://dx.doi.org/10.1016/j.rser.2014.07.179
1364-0321/© 2014 Elsevier Ltd. All rights reserved.

5.3.2. Applications of microencapsulated phase change materials in engineering project. . . . 256
6. Conclusions and outlook . . . 256
Acknowledgments . . . 257
References . . . 257

1. Introduction

Latent heat storage is one of the most efficient ways to store thermal energy. The advantages of the latent heat storage (LHS) in comparison with sensible storage are high heat storage density, small size of the system, and a narrow temperature change during charging and discharging processes. In the latent heat storage system, thermal energy is stored in phase change materials (PCMs) during a melting process while it is recovered during a freezing process [1]. PCMs have received attention for various applications such as waste heat recovery systems, solar heating systems, building energy conservation systems and air-conditioning systems [2,3].

In solar heating systems, heat energy can be stored in PCMs, which may provide much higher energy storage density with a smaller temperature swing when compared with the sensible heat storage. The volume of heat storage tank may be decreased, so the cost of the solar heating system can be reduced accordingly. The application of cool storage air-conditioning systems shifts daytime air-conditioning loads to nighttime hours when the cooling load is low. Daytime cooling can be supplied by circulating the cooling medium rather than operating the compressor. Benefits can be received by both the consumer (lower energy costs, better space temperature control) and the utility (higher load factor, lower capital investment in new generating equipment) [4].

Many inorganic and organic PCMs (salt hydrates, fatty acids/esters, paraffin waxes, etc.) and PCM mixtures have been studied for thermal energy storage applications [5,6]. However, they need encapsulation in order to prevent leakage of the melted PCM during the phase change process. Now, these problems can be solved by using shape-stabilized PCMs. These shape-stabilized PCMs can be prepared by integrating the PCMs into the supporting material and microencapsulating the PCMs into the shell. The shape-stabilized PCMs are mainly classified as composite PCMs and microencapsulated PCMs. The shape-stabilized PCMs are usually fabricated by embedding PCMs into shape stabilization supports such as high density polyethylene (HDPE), styrene, butadiene, polymethacrylic acid, polystyrene resin, etc. The PCMs and the supporting material are melted by heating the supporting material over the glass transition temperature, and mixed with each other at high temperature. The melted mixtures are cooled to room temperature until they become solid. The shape-stabilized PCMs can keep the shape stabilized during phase transition process, and do not need container for encapsulation. Fig. 1 shows the type of shape-stabilized thermal energy storage materials. A number of preparation and thermal properties investigations have been performed on the shape-stabilized thermal energy storage materials. Therefore, a review on preparation, thermal properties and applications of the shape-stabilized thermal energy storage materials is presented in this paper.

2. Preparation and thermal properties of composite phase change materials

The composite PCMs can be prepared by integrating the PCMs into the supporting material. The supporting material is classified as inorganic supporting material and organic supporting material. Some preparation and thermal properties investigations on the composite PCMs with two types of supporting material have been carried out in recent years.

2.1. Composite phase change materials with organic supporting material

The use of fatty acids such as stearic acid (SA), palmitic acid (PA), myristic acid (MA), and lauric acid (LA) as shape-stabilized PCMs increases their feasibilities in practical latent heat storage applications. A series of fatty acid/poly (methyl methacrylate) (PMMA) blends, such as SA/PMMA, PA/PMMA, MA/PMMA, and LA/PMMA were prepared as new kinds of shape-stabilized PCMs by encapsulating fatty acids into PMMA which acted as supporting material. The fatty acids/PMMA blends were prepared by the solution casting method. Solutions of PMMA and one of the fatty acids in chloroform were prepared in separate beakers and fatty acid solution was added to PMMA solution drop by drop. The blends were prepared at different mass fraction of fatty acids (50, 60, 70, 80, and 90% w/w) to reach maximum encapsulation ratio. Thermal properties of the

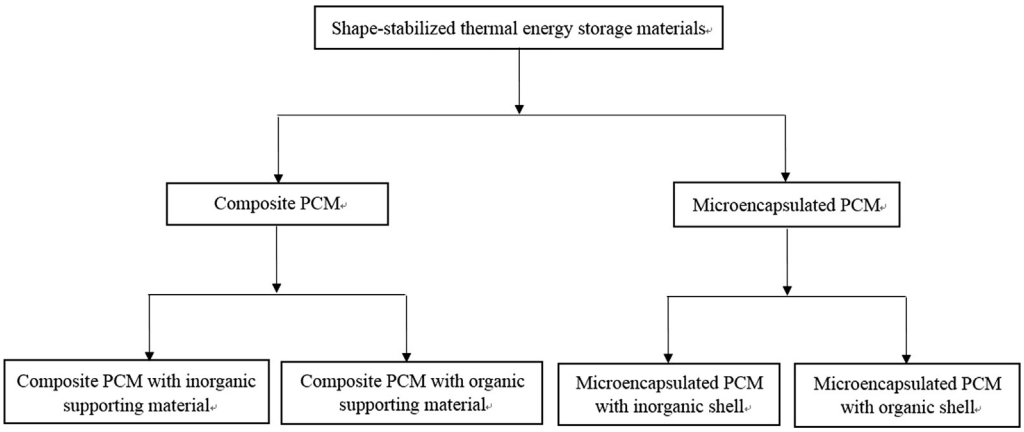


Fig. 1. The type of shape-stabilized thermal energy storage materials.

prepared fatty acid/PMMA (80/20 wt%) blends as shape-stabilized PCMs were measured using differential scanning calorimeter (DSC). The DSC results indicated that the melting latent heats of the shape-stabilized SA/PMMA, PA/PMMA, MA/PMMA and LA/PMMA (80/20 wt %) blends are 187.72, 173.89, 166.56 and 149.55 kJ/kg, and the freezing latent heats are 190.34, 175.53, 168.81 and 151.32 kJ/kg, respectively. It is also observed that the melting points of the shape-stabilized SA/PMMA, PA/PMMA, MA/PMMA and LA/PMMA (80/20 wt %) blends are 67.31, 59.98, 51.00 and 40.96 °C, and the freezing points are 66.78, 59.35, 50.74 and 41.55 °C, respectively. It could be concluded that the shape-stabilized fatty acid/PMMA blends have high latent heat storage capacity and proper phase change temperatures at range of 40–70 °C for practical latent heat storage applications such as under floor space heating and absorbing solar energy in wallboard, plaster board or floor impregnated with the shape-stabilized PCMs [7].

The ultra fine fibers of lauric acid/polyethylene terephthalate (LA/PET) composite (1:1, w/w) were successfully prepared. In the preparation process, a 15 wt% PET solution was prepared by dissolving the PET in a mixture of dichloromethane (DCM) and trifluoroacetic acid (TFA) (2/1, v/v) and selected as the original solution for the quicker dissolving speed of PET and the good quality of the electrospun fibers. Then, LA with the equal weight of PET was added to the PET solution (LA/PET=1/1, w/w) under constant stirring for 1 h. During the electrospinning, the solution was placed in a 5 ml syringe and was fed by a syringe pump at a rate of 3 ml/h. The fibers were dried in vacuum at room temperature for 24 h to remove residual solvent. The results indicated that the electrospun fibers are cylindrical shape with smooth surface and the average fiber diameter is about 710 nm. It is found that the melting and crystallization latent heats of the shape-stabilized LA/PET composite fibers are 70.76 and 62.14 kJ/kg, and the melting and crystallization points are 45.14 and 38.57 °C. The results showed that the shape-stabilized LA/PET composite fibers have the potential applications in solar energy storage and thermo-regulating textile [8].

A kind of shape-stabilized PCMs based on high density polyethylene (HDPE)/ethylene-vinyl acetate (EVA) alloy, organophilic montmorillonite (OMT), paraffin and intumescent flame retardant (IFR) were prepared using twin-screw extruder technique. The HDPE–EVA alloy/OMT nanocomposites acted as the supporting material and formed the three-dimensional network structure. The paraffin was used as a phase change material and dispersed in the three-dimensional network structure. The DSC results indicated that the phase change peaks of the paraffin occurred in shape-stabilized PCMs. The molten peak of HDPE was also presented at around 127 °C. It is noted that the additives of IFR had little effect on the network structure and the latent heat of shape-stabilized PCMs. The thermogravimetric analyzer (TGA) was used to determine the thermal stability of the shape-stabilized PCMs. The TGA analysis results showed that the flame retardant shape-stabilized PCMs produced a larger amount of char residue at 800 °C than that of the shape-stabilized PCMs [9].

The 1-tetradecanol (TD)/1,3:2,4-di-(3,4-dimethyl) benzylidene sorbitol (DMDBS) composite was prepared as a shape-stabilized PCM by impregnating DMDBS into TD and the maximum weight percentage of TD is up to 94.2 wt%. The DSC results showed that the melting and freezing enthalpies of 1-tetradecanol in the composite PCM are 218.5 and 215.3 kJ/kg. The DMDBS three-dimensional network trapped and immobilized most of the 1-tetradecanol. So, the gel-to-sol transition temperature of the composite PCM increased to 158.3–180.0 °C and the 1-tetradecanol leakage decreased [10].

The shape-stabilized PCMs based on cellulose, agarose, and chitosan as matrix polymers and PEG as PCM were prepared in melt for latent heat storage applications in solar space heating and ventilating systems in buildings. The PEG/cellulose (60/40% w/w), PEG/agarose (70/30% w/w) and PEG/chitosan (80/20% w/w) blends were found to contain maximum PEG without leakage above melting point. The DSC results showed that the shape-stabilized PEG/cellulose, PEG/agarose and PEG/chitosan composites melt at 58.51 °C, 57.73 °C and 57.18 °C with latent heats of 84.63 kJ/kg, 110.87 kJ/kg and 152.16 kJ/kg, while they crystallize at 37.05 °C, 43.36 °C and 44.76 °C with latent heats of 78.92 kJ/kg, 99.01 kJ/kg and 138.39 kJ/kg [11].

The paraffin/high density polyethylene (HDPE) composites as shape-stabilized PCMs were prepared by mixing the melted paraffin with the melted HDPE and cooling to room temperature. In this preparation process, two kinds of paraffins with melting temperatures of 42–44 °C (type P1) and 56–58 °C (type P2) and latent heats of 192.8 kJ/kg and 212.4 kJ/kg were used. The maximum weight percentage for both paraffin types in the composite PCMs without any seepage of the paraffin in the melted state were found to be 77%. The DSC results indicated that the melting temperatures and latent heats of the shape-stabilized P1/HDPE and P2/HDPE composite PCMs are 37.8 °C and 55.7 °C, and 147.6 kJ/kg and 162.2 kJ/kg, respectively. The thermal conductivity of the P1/HDPE and P2/HDPE is increased about 14% and 24% by adding expanded and exfoliated graphite (EG) into the composite PCMs in the ratio of 3 wt% [12].

The ultrafine composite fibers based on the composites of binary fatty acid eutectics and polyethylene terephthalate (PET) with varied fatty acid eutectics/PET mass ratios (50/100, 70/100, 100/100 and 120/100) were prepared using the technique of electrospinning as shape-stabilized PCMs. The five binary fatty acid eutectics including LA–MA, LA–PA, MA–PA, MA–SA and PA–SA were used as solid–liquid PCMs. The scanning electronic microscope (SEM) was employed to examine the morphology and microstructure of the shape-stabilized PCMs. The SEM photograph showed that the electrospun binary fatty acid eutectics/PET ultrafine composite fibers have the wrinkled surfaces morphologies compared with the neat PET fibers with cylindrical shape and smooth surfaces. The DSC results indicated that the heat enthalpies of melting and crystallization of the ultrafine composite fibers increase gradually with increasing fatty acid eutectics amounts, but their phase transition temperatures have almost no obvious variation as compared to the corresponding fatty acid eutectics [13].

The fatty acid eutectics/PMMA as shape-stabilized PCM was successfully prepared by the method of self-polymerization. By introducing the binary fatty acid eutectics, phase change temperatures of the composites CA–LA/PMMA, CA–MA/PMMA, CA–SA/PMMA and LA–MA/PMMA (50/50 wt%) were adjusted to the suitable range for building energy conservation (ranging from 21 °C to 35 °C). The LA–MA eutectic/PMMA was used to investigate the feasible maximum composition ratio of the shape-stabilized PCMs. The feasible maximum mass fraction of LA–MA eutectic was found to be 70%. The DSC results indicated that phase change temperatures of the CA–LA/PMMA, CA–MA/PMMA, CA–SA/PMMA and LA–MA/PMMA composites are 21.11 °C, 25.16 °C, 26.38 °C and 34.81 °C and their latent heat values are 76.3 kJ/kg, 69.32 kJ/kg, 59.29 kJ/kg and 80.75 kJ/kg, respectively [14].

The poly (ethylene glycol) (PEG)/silsesquioxane composites were prepared by in situ sol–gel process. The leakage phenomenon of PEG was inhibited due to the mesoporous confinement of supporting matrix. The DSC results showed that the latent heat of the shape-stabilized PCMs is 124.7 kJ/kg and the main melting point is 56.4 °C, and the composite PCMs still have large latent heat of 124.1 kJ/kg after 1000 thermal cycles. The thermal stability and flame retardancy properties of the composite PCMs were significantly improved due to the inorganic–organic hybrid fire-resistance supporting matrix. The composite PCMs have large latent heat, good fire resistance and thermal reliability for thermal energy storage application [15].

The shape-stabilized PCM was prepared by incorporating dodecyl alcohol (DA) into ground granulated blast furnace slag (GGBS) through vacuum impregnation. Fig. 2 illustrates the vacuum impregnation system. The results indicated that the maximum percentage of DA retained in GGBS is 11% without seepage. The DSC results showed that the melting and freezing temperatures of the composite PCM are 21.16 °C and 19.10 °C, respectively while the latent heats of melting and freezing are 22.51 kJ/kg and 21.62 kJ/kg, respectively. The TGA results confirmed that the composite PCM is thermally stable and reliable. It is concluded that the shape-stabilized PCM is a potential candidate for thermal energy storage in buildings [16].

The ultrafine fibers based on the composites of polyethylene terephthalate (PET) and a series of fatty acids, such as lauric acid (LA), myristic acid (MA), palmitic acid (PA), and stearic acid (SA), were prepared by electrospinning as shape-stabilized PCMs.

Fig. 3 shows that the SEM photograph of electrospun fatty acids/PET composite fibers with same mass ratio (70/100). The SEM results indicated that the four fatty acid/PET composite ultrafine fibers are cylindrical in shape with smooth surface, and the average diameter of the composite fibers increase with the increase of alkyl chain of the fatty acid in the composite fibers. The DSC results showed that the latent heats of fusion are about 54.91, 60.99, 66.91 and 67.88 kJ/kg for LA/PET, MA/PET, PA/PET and SA/PET composite fibers with the fatty acid/PET mass ratio of 70/100, respectively, while the latent heats of crystallization are about 51.93, 55.93, 58.65 and 61.62 kJ/kg, respectively. So, this result indicated that both of the latent heat and phase transition temperature of the PCM/polymer composite fibers are dominantly related with the type of PCMs [17].

The heat conduction enhanced shape-stabilized PCMs were prepared by mixing the melted paraffin with the melted high density polyethylene (HDPE) at about 160 °C (the mass proportion of paraffin and HDPE was 80:20), then adding thermal conductivity enhanced additives to the melted composite samples with stirring for 20–30 min, and finally cooling the melted shape-stabilized PCMs to room temperature. The obtained heat conduction enhanced shape-stabilized PCMs are shown in Fig. 4. The experimental results indicated that the thermal conductivities of the shape-stabilized paraffin/HDPE composite PCMs could be improved by addition of expanded graphite (EG). The thermal conductivity of the PCM is up to 1.36 W/m K as the addition of EG is in the ratio of 4.6 wt%, which is much better than that by addition of graphite powder (GP). The latent heat of the heat conduction enhanced PCMs decreased little due to small amount of EG, and good uniformity structure was observed by SEM [18].

The capric acid (CA)/halloysite nanotube (HNT) composites were prepared as a shape-stabilized PCMs. The composite PCMs contained capric acid as high as 60 wt% and maintained its original shape without any leakage of capric acid after subjected to 50 melt-freeze cycles. The DSC results showed that the melting temperature and latent heat of composite PCMs (CA/HNT: 60/40 wt%) are 29.34 °C and 75.52 kJ/kg. The thermal storage and release rates could be increased by 1.8 and 1.7 times, respectively, by addition of graphite. From these results, it is concluded that the shape-stabilized CA/HNT composite could be used as candidate PCM for thermal energy storage applications such as solar energy storage, building energy conservation and agricultural greenhouse [19].

Electrospun polyacrylonitrile (PAN) nanofibrous mats and the derived carbon nanofibrous mats were studied to prepare shape-stabilized PCMs with fatty acid eutectics for storage and retrieval of thermal energy. The carbon mats were made from the PAN mats through stabilization in air followed by carbonization in nitrogen. Three fatty acid eutectics of capric acid–lauric acid, capric acid–palmitic acid, and capric acid–stearic acid were used as PCMs. The prepared fatty acid eutectics (CA–LA, CA–PA, and CA–SA) were placed in a beaker at 60 °C until being melted completely. The PAN and carbon nanofibrous mats were cut into specimens with sizes of 5 cm × 5 cm. Thereafter, the specimens were immersed into molten fatty acid eutectics for 10 h until the absorption was saturated. Finally, the nanofibrous mats absorbed with fatty acid eutectics were hung in an oven at 60 °C for 10 h. The results showed that electrospun nanofibrous mats are highly porous and capable of absorbing a large amount of PCMs, and the maximum

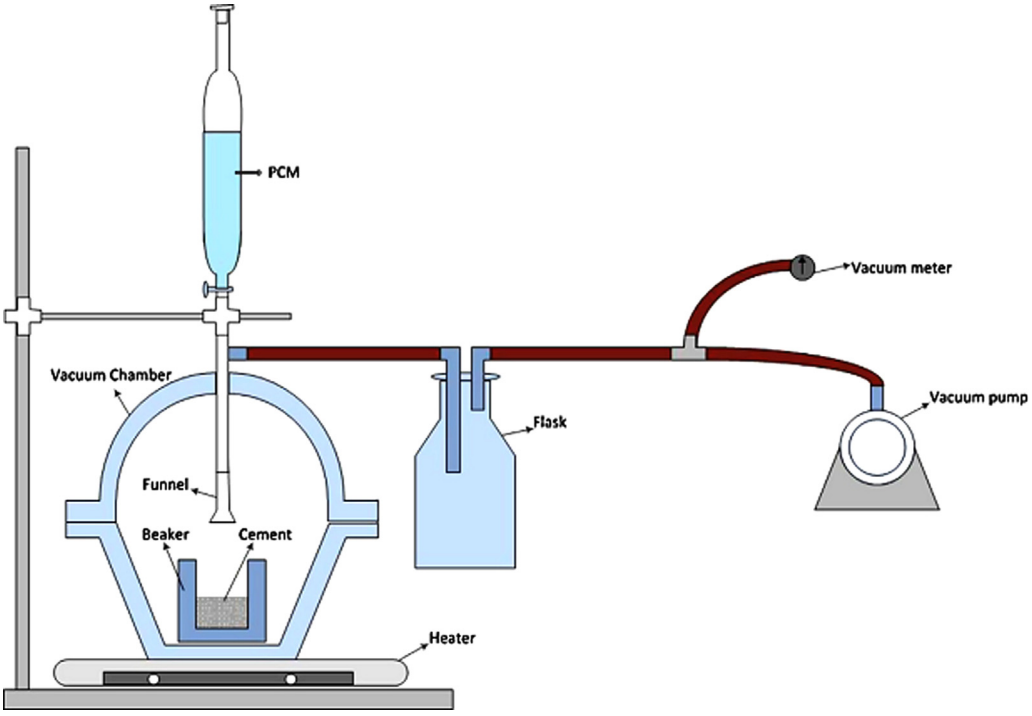


Fig. 2. Schematic diagram of vacuum impregnation system [16].

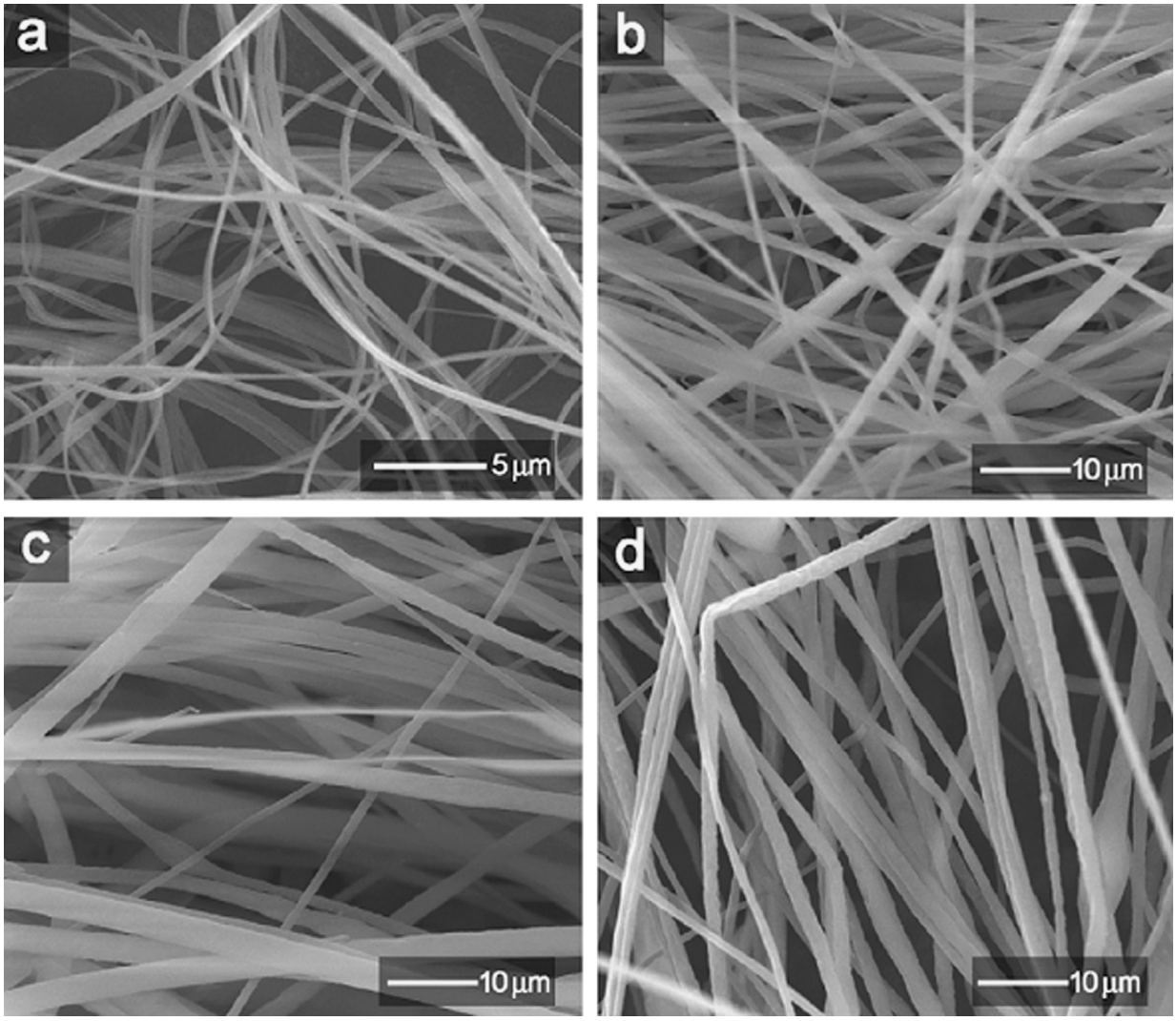


Fig. 3. SEM photograph of electrospun fatty acids/PET composite fibers with same mass ratio (70/100): (a) LA/PET, (b) MA/PET, (c) PA/PET and (d) SA/PET [17].

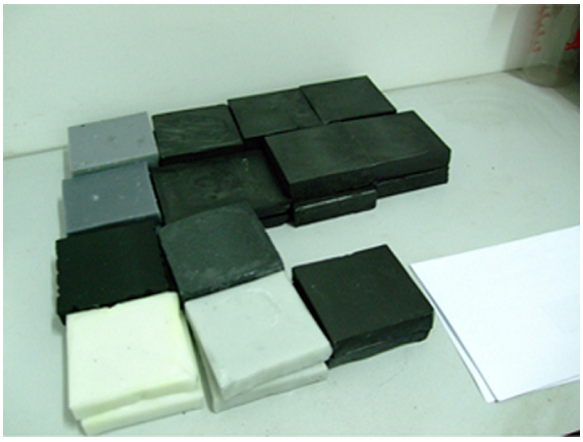


Fig. 4. Photograph of the shape-stabilized PCMs [18].

absorption capacities of PAN and carbon mats are about 99 wt% and 81 wt%, respectively. The DSC results indicated that the melting temperatures and enthalpies of the prepared composite PCMs are in the range of 19.8–31.4 °C and 120.1–165.4 kJ/kg for PAN mats, and 18.8–30.7 °C and 92.1–128.0 kJ/kg for carbon mats. The melting times of CA–PA/carbon and freezing times of CA–SA/carbon were shortened by about 49.5% and 41.0%, respectively, as compared to melting times of CA–PA/PAN and freezing times of CA–SA/PAN. It is concluded that the shape-stabilized PCMs could be utilized for potential applications in building energy conservation [20].

The myristic acid (MA)/polyaniline (PANI) shape-stabilized PCMs were prepared by means of the surface polymerization method. The MA and PANI were used as thermal energy storage material and supporting material, respectively. The PANI particles that polymerized from aniline were deposited on the surface of MA particles to form the shape-stabilized PCM. The TGA results indicated that the shape-stabilized PCM have good thermal stability when the phase change process occurred. The DSC results revealed that the phase change enthalpy of the shape-stabilized PCM is increased linearly with the increase of the MA loading. The highest loading of the MA in the shape-stabilized PCM with good stability is 82 wt%, corresponding to the phase change enthalpy of 150.63 kJ/kg [21].

The shape-stabilized PCMs with high thermal conductivity were prepared by using organic n-octadecane as phase change material, high density polyethylene (HDPE) as support material, and EG as thermal conductivity enhancer. The test results indicated that adding a small amount of EG could significantly improve thermal conductivity of the PCMs almost without effect on its thermal storage capacity and phase change temperature.

When the mass fraction of EG is 5%, thermal conductivity is 1.76 W/(m K), which is over 4 times than that of the original one. When the EG content varies from 1 wt% to 5 wt%, the biggest change of latent heat is 6.4%, and the phase change temperature is 20.1 °C, 21.7 °C, 22.1 °C and 20.3 °C, correspondingly [22].

2.2. Composite phase change materials with inorganic supporting material

The capric acid (CA)–myristic acid (MA) eutectic mixture/vermiculite (VMT) composites were prepared as a shape-stabilized PCMs using vacuum impregnation method. The CA–MA eutectic mixture could be retained by 20 wt% into pores of the VMT without melted PCMs seepage from the composite. The thermal cycling test indicated that the shape-stabilized PCMs have good thermal reliability and chemical stability although it was subjected to 3000 melting/freezing cycling. The thermal conductivity of the shape-stabilized CA–MA/VMT composite PCMs is increased by about 85% by adding 2 wt% expanded graphite (EG) into the composite. The DSC results showed that the melting and freezing temperatures of the shape-stabilized CA–MA/VMT composite are 19.75 °C and 17.05 °C, respectively, and the melting and freezing latent heats of the shape-stabilized PCM are 27.46 kJ/kg and 31.42 kJ/kg, respectively [23].

The shape-stabilized PCMs were prepared by vacuum impregnation of paraffin within graphene oxide (GO) sheets. The composite PCMs contained 48.3 wt% of paraffin without leakage of melted PCMs. The SEM results indicated that the paraffin was bounded into the pores of GO. The DSC results showed that the melting and freezing temperature of the shape-stabilized PCM are 53.57 °C and 44.59 °C, and the melting and freezing latent heats of the shape-stabilized PCM are 63.76 kJ/kg and 64.89 kJ/kg, respectively. The thermal cycling tests verified that the shape-stabilized PCMs have good thermal reliability and chemical stability. The thermal conductivity of the shape-stabilized PCMs can be improved from 0.305 W/m K to 0.985 W/m K. From these results, it is concluded that the prepared paraffin/GO composite is appropriate PCM for thermal energy storage applications [24].

Several building composite PCMs (BCPCMs) were prepared by blending of liquid xylitol pentalaurate (XPL) and xylitol pentamyristate (XPM) esters with gypsum, cement, diatomite, perlite and vermiculite as supporting matrices. The test results indicated that the highest adsorption ratio of XPL ester into gypsum, cement, perlite, diatomite, and vermiculite was 20, 19, 71, 52 and 40 wt%, respectively while it was 22, 25, 66, 50 and 41 wt% for XPM ester, respectively. The DSC results showed that the melting temperatures and latent heats of the prepared BCPCMs are in range of 40–55 °C and 31–126 kJ/kg, respectively. The TG results indicated that the BCPCMs have good thermal endurance even above their phase change temperatures. The BCPCMs also presented almost same chemical and phase change characteristics after 1000 thermal cycling test [25].

The shape-stabilized paraffin/silicon dioxide (SiO_2)/expanded graphite (EG) composite PCM was prepared by the sol–gel method. Silica gel acted as the supporting material and EG was used to increase the thermal conductivity. The mass fractions of the SiO_2 and EG were 20.8% and 7.2%, respectively. The DSC results showed that the phase change temperatures of the paraffin/SiO_2 composite and the paraffin/SiO_2/EG composite are 27.53 °C and 27.72 °C, respectively, and the latent heats of the paraffin/SiO_2 composite and the paraffin/SiO_2/EG composite are 112.8 kJ/kg and 104.4 kJ/kg, respectively. The test results indicated that thermal conductivity of the SiO_2/paraffin composite and the SiO_2/paraffin/EG composite are 28.2% and 94.7% higher than that of paraffin (0.1264 W/m K), respectively [26].

The shape-stabilized lauric acid (LA)/silicon dioxide (SiO_2) composite PCMs were prepared using sol–gel methods. The LA was used as the phase change material for thermal energy storage, and the SiO_2 acted as the supporting material. The SEM results showed that the LA was well dispersed in the porous network of SiO_2. The DSC results indicated that the LA/SiO_2 composite PCMs solidify at 41.30 °C with a latent heat of 90.00 kJ/kg and melt at 42.46 °C with a latent heat of 117.21 kJ/kg when the mass percentage of the LA in the SiO_2 is 64.8%. The TGA results presented that the shape-stabilized LA/SiO_2 composite PCMs have good thermal stability. The shape-stabilized PCMs can be used for thermal energy storage in waste heat recovery and solar heating systems [27].

The shape-stabilized polyethylene glycol (PEG)/silicon dioxide (SiO_2) composite PCM was prepared by dissolving SiO_2 and PEG in water with quick continuous stirring for 12 h. The PEG was used as the latent heat storage material and the SiO_2 acted as the supporting material, which provided structural strength and prevented the leakage of the melted PEG. The test results indicated that the composite PCM remained solid when the weight percentage of the SiO_2 was higher than 15%. The DSC results showed that the PEG (85%)/SiO_2 composite PCM has a large enthalpy of 162.9 kJ/kg and suitable melting temperature of 61.61 °C. In order to consider the suitable enthalpy value and conductivity of the composite PCM, the combination percentage for composite PCM is about PEG (80%)/SiO_2 (20%). In this composite PCM, the latent heat of the composite PCM is 137.7 kJ/kg and the thermal conductivity for the composite PCM is increased by 21% [28].

Flame retardant n-hexadecane/silicon dioxide (SiO_2) composite PCMs were prepared using sol–gel methods. In the composites, n-hexadecane was used as the PCM for thermal energy storage, and SiO_2 acted as the supporting material that is fire resistant. In order to further improve flame retardant property of the composites, the expanded graphite (EG) was added in the composites. The SEM results showed that then-hexadecane was well dispersed in the porous network of the SiO_2. The DSC results indicated that the composites solidify at 16.07 °C with a latent heat of 145.10 kJ/kg and melt at 20.08 °C with a latent heat of 147.58 kJ/kg as the mass percentage of n-hexadecane in the composites is 73.3%. The TGA results showed that the loading of the EG increased the charred residue amount of the composites at 700 °C, contributing to the improved thermal stability of the composites. It is observed from SEM photographs that the homogeneous and compact charred residue structure after combustion improved the flammability of the composites [29].

The capric–palmitic acid/attapulgite composite PCMs were prepared by the vacuum method. The capric–palmitic could be absorbed uniformly into attapulgite and the optimum absorption ratio of capric–palmitic binary fatty acid was 35%. There was no chemical reaction between the capric–palmitic acid and attapulgite. The DSC results indicated that the phase change temperature of the capric–palmitic acid/attapulgite composite PCM is 21.71 °C and the latent heat is 48.2 kJ/kg [30].

The stearic acid (SA)/expanded graphite (EG) composites with different mass ratios were prepared by absorbing liquid SA into the EG. In the composite materials, the SA was used as the PCM for thermal energy storage, and the EG acted as the supporting material. The DSC results showed that the SA/EG composites solidify at temperature of 54.28 °C with latent heat of 155.70 kJ/kg, and melt at temperature of 53.12 °C with latent heat of 155.50 kJ/kg when the mass percentage of the SA in the composites is up to 83%. The thermal diffusivity of the composites is 10 times higher than that of the SA. The SA was well dispersed in the porous network of the EG by capillary and surface tension forces, so the leakage of the melted SA from the composites can be prevented even when it was heated above the melting temperature of the SA [31].

The shape-stabilized palmitic acid (PA)/graphene oxide (GO) composite PCMs were prepared by the vacuum impregnation method. The GO was used as supporting material to improve thermal conductivity and shape stabilization of composite PCM. The DSC results indicated that the melting and freezing temperatures of the composite PCM are 60.45 °C and 60.05 °C, respectively, and the melting and freezing latent heats of the composite PCM are 101.23 kJ/kg and 101.49 kJ/kg, respectively. The test results showed that the composite PCMs have a good thermal reliability in terms of thermal properties and chemical stability after 2500 melting/freezing cycles. Thermal conductivity of the composite PCM is improved from 0.21 W/m K to 1.02 W/m K [32].

The shape-stabilized palmitic acid (PA)/active aluminum oxide composite PCMs were prepared by adsorbing liquid palmitic acid into active aluminum oxide. The SEM results showed that the PA was well adsorbed into porous network of the active aluminum oxide. The DSC results indicated that the composites melt at 60.25 °C with a latent heat of 84.48 kJ/kg and solidify at 56.86 °C with a latent heat of 78.79 kJ/kg when the mass ratio of the PA to active aluminum oxide is 0.9:1. The EG can increase thermal conductivity of the composites, so the melting and solidifying times of the CPCM5 are decreased by 20.6% and 21.4% compared with that of the PA. The active aluminum oxide can improve thermal stability of the composites due to the synergistic effect between the PA and active aluminum oxide [33].

The fatty acid ester/building material composites as shape-stabilized PCMs were prepared by absorbing liquid fatty acid esters into porous network of conventional building materials. In the composites, erythritol tetrapalmitate (ETP) and erythritol tetrastearate (ETS) esters were used as PCM for thermal energy storage, and cement and gypsum acted as supporting material. The maximum weight percentage of the ester compounds confined in the cement and the gypsum was 18% for cement based-composite and 22% gypsum based-composite. The SEM results showed that the esters were confined in the porous network of the cement and gypsum. The DSC results indicated that the melting temperatures and the latent heats of the prepared composite PCMs are in range of 21.6–32.3 °C and 35.9–43.3 kJ/kg, respectively. The thermal cycling test presented that the composite PCMs have good thermal reliability, chemical and structural stability even after 1000 thermal cycling. The TGA analysis results revealed that the composite PCMs have good thermal stability. From all results, it can be concluded that the shape-stabilized composites are promising PCMs for thermal energy storage in building applications [34].

The palmitic acid (PA)/expanded graphite (EG) composites as shape-stabilized PCMs were prepared by using vacuum impregnation system. The maximum mass fraction of the PA retained in EG was 80 wt% without the leakage of the PA in melted state even when it was heated over the melting point of the PA. From DSC analysis, the melting and freezing temperatures and latent heats of the form-stable PCM were determined to be 60.88 °C and 60.81 °C and 148.36 kJ/kg and 149.66 kJ/kg, respectively. Thermal cycling test indicated that the composite PCMs have good thermal reliability after 3000 melting/freezing cycles. The Fourier transformation infrared spectroscope (FT-IR) was used to analyze the chemical structure. The FT-IR results revealed that it has good chemical stability after thermal cycling. The test results presented that the thermal conductivity of shape-stabilized PA/EG (80/20 w/w%) composite (0.60 W/m K) is 2.5 times higher than that of pure PA (0.17 W/m K) [35].

The n-octadecane/molecular sieve 5A composites as shape-stabilized PCMs were prepared by adsorbing liquid n-octadecane into the molecular sieve 5A. In the composites, the n-octadecane was used as thermal storage material, and the molecular sieve 5A acted as the supporting material. The DSC results of the n-octadecane, FPCM1, FPCM2, FPCM3, FPCM4 and FPCM5 are illustrated in Fig. 5. The DSC results indicated that the shape-stabilized PCMs melt at 28.33 °C with a latent heat of 101.14 kJ/kg and solidify at 26.75 °C with a latent heat of 97.55 kJ/kg when maximum appropriate mass percentage of the n-octadecane in the composites is about 33.3%. The differences between melting temperature and solidifying temperature of the n-octadecane, FPCM1–FPCM5 are 3.02 °C, 1.22 °C, 1.27 °C, 1.49 °C, 1.58 °C and 1.33 °C, correspondingly. This result indicates that the supercooling degree of the FPCM1, FPCM2, FPCM3, FPCM4 and FPCM5 is smaller than that of the n-octadecane during solidification process owing to porous wall of the molecular sieve 5A acted as nucleation agent. The TGA results revealed that there is a two-step thermal degradation process. The first step degradation takes place at the temperature between 100 °C and 220 °C, which corresponds to the thermal degradation of the n-octadecane molecular chains. The second step degradation occurs from 280 °C to 400 °C, which represents the thermal degradation of the molecular sieve 5A [36].

The polyethylene glycol (PEG)/diatomite composites as shape-stabilized PCMs were prepared by incorporating PEG in the pores of diatomite. The PEG can be retained by 50 wt% into pores of the diatomite without the leakage of melted PEG from the composite. The DSC results showed that the melting and freezing temperatures and latent heats of the composite PCM are 27.70 °C and 32.19 °C, and 87.09 kJ/kg and 82.22 kJ/kg, respectively. Thermal cycling test indicated that the composite PCMs have good thermal and chemical reliability after 1000 melting/freezing cycling. The TGA analysis revealed that the PEG in the composite has as good thermal stability

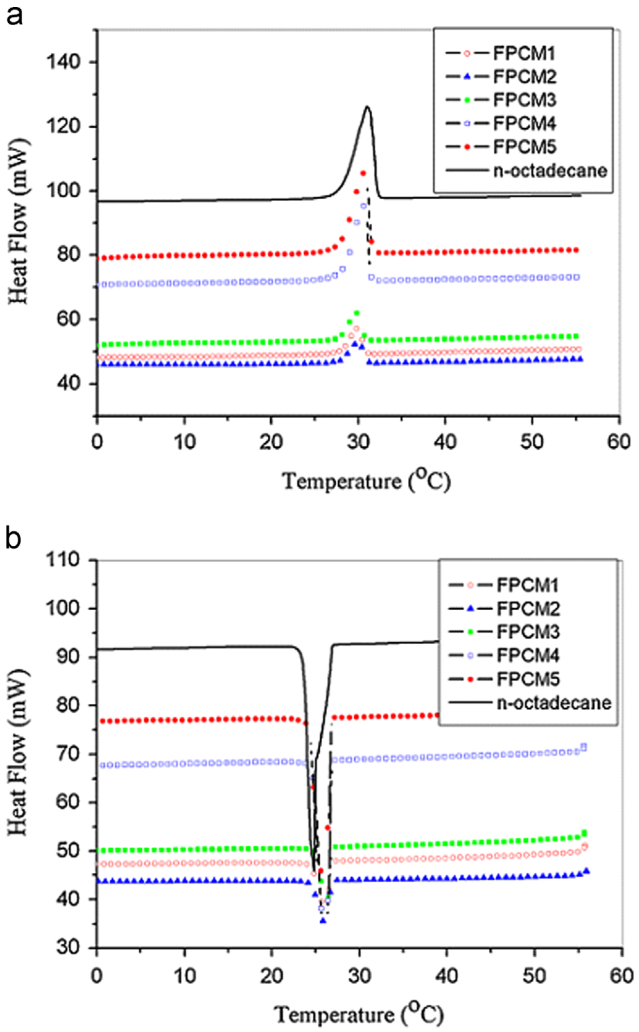


Fig. 5. DSC curves of the n-octadecane, FPCM1–FPCM5 (a) the melting process and (b) the solidifying process [36].

as pure PEG even after thermal cycling. The test results also showed that the thermal conductivity of the diatomite/PEG composite PCM is increased as 28%, 50%, 78% and 103% by addition of EG in mass fraction 3%, 5%, 8% and 10%, respectively [37].

The palmitic acid/silicon dioxide (SiO_2) composites with flame retardant as thermal energy storage PCMs were prepared using sol–gel methods. In the composites, palmitic acid was used as the PCM for thermal energy storage, and SiO_2 acted as the supporting material. The SEM results showed that palmitic acid was well dispersed in the porous network of the SiO_2. The DSC results indicated that the composites solidify at 59.20 °C with a latent heat of 60.55 kJ/kg and melt at 59.76 °C with a latent heat of 85.11 kJ/kg when the mass percentage of the palmitic acid in the composites is 41.1%. The TGA results presented that addition of melamine improved thermal stability and flame retardant property. The microstructure of the charred residue after combustion indicated that the homogeneous and compact charred residue decreased the flammability of the composites [38].

The capric–myristic acid (CA–MA)/expanded perlite (EP) composites as shape-stabilized PCMs were prepared by incorporating eutectic mixture of the CA and MA into the EP. The maximum CA–MA absorption of the EP was determined to be 55 wt% without melted PCM seepage from the composite. The DSC analysis results indicated that the temperatures of melting and freezing and latent heats of melting and freezing of the shape-stabilized CA–MA/EP composite PCMs are 21.70 °C, 20.70 °C, and 85.40 kJ/kg, 89.75 kJ/kg, respectively. Thermal cycling test revealed that the shape-stabilized composite PCMs have good thermal reliability in terms of thermal properties after 5000 thermal cycling. The test results showed that the thermal conductivity of the shape-stabilized PCMs is increased about 58% by the addition of 10 wt% expanded graphite (EG) [39].

The n-nonadecane/cement composites as thermal energy storage materials were prepared by absorbing n-nonadecane in porous network of cement. In composite materials, n-nonadecane was used as the PCM for thermal energy storage, and cement acted as the supporting material. The SEM results showed that the n-nonadecane was well dispersed in the porous net-work of cement. The DSC results indicated that the n-nonadecane/cement composite material has the melting latent heat of 69.12 kJ/kg with melting temperature of 31.86 °C, and solidifying latent heat of 64.07 kJ/kg with solidifying temperature of 31.82 °C. The TGA results revealed that the n-nonadecane/cement composites have good thermal stability and can be used repeatedly in buildings [40].

The shape-stabilized stearic acid (SA)/graphene oxide (GO) composites were prepared by imprisoning the SA into the interlayer spaces of the multilayer GO. The leakage of the melted SA from the composites was prevented, and the GO can improve thermal stability of the composites because the carbonaceous layers create a physical protective barrier on the surface of the composites. The DSC results showed that the melting and freezing temperatures of the SA are 74 °C and 57 °C, and the melting latent heat is 140.9 kJ/kg. It is also found that the melting and freezing temperatures of the SA/GO composite with SA/GO mass ratio of 1 are 33 °C and 23 °C, and the melting and freezing enthalpy values are 55.7 kJ/kg and 55.9 kJ/kg, respectively [41].

The shape-stabilized lauric acid/activated carbon composites as PCMs were prepared by adsorbing liquid lauric acid into activated carbon. The DSC results indicated that the shape-stabilized LA/activated carbon composites melt at 44.07 °C with a latent heat of 65.14 kJ/kg and solidify at 42.83 °C with a latent heat of 62.96 kJ/kg when the maximum mass percentage of the LA in the composites is 33.3%. The supercooling degree of the composites is smaller than that of the LA during solidification due to the porous wall of the activated carbon acting as nucleation agent. The thermal conductivity of the composites with EG in the solidifying state and melting state is increased by 4.67% and 71.1%, respectively, in comparison with the thermal conductivity of the composites without EG. Fig. 6 displays the TGA curves of the LA, and PCM1–PCM4. As shown in Fig. 6, there are two-step thermal degradation processes: the first step happens at a temperature between 120 °C and 250 °C, corresponding to the thermal degradation of the LA molecular chains, and the second step occurs from 300 °C to 450 °C, representing the thermal degradation of the activated carbon. The activated carbon can improve thermal stability of the composites as to the carbonaceous layers create a physical protective barrier on the surface of the composites [42].

2.3. Comparison of composite phase change materials with organic and inorganic supporting material

The shape-stabilized composite PCMs can be prepared by integrating the PCMs into the supporting material. The manufacturing efficiency of the composite PCMs depends on adsorption ability of the supporting material. Multi-pores structures of the supporting material result in large specific surface area. This is propitious to absorb liquid PCMs into porous network of the supporting material. Table 1 presents the comparison of composite phase change materials with organic and inorganic supporting material. As shown in Table 1, the higher mass ratio of the PCMs in the composites, the larger latent heat of the composite PCMs.

3. Preparation and thermal properties of microencapsulated phase change materials

The shape-stabilized PCMs can be prepared by microencapsulating the PCMs into the shell. Microencapsulated PCMs can be achieved by physical method such as spray-drying and the chemical method such as complex coacervation, interfacial polycondensation and in-situ polymerization. Various materials are chosen to prepare the shell of the microencapsulated PCMs, such as amino plastics, gelatin-gum Arabic, gelatin, melamine formaldehyde and polymethylmethacrylate. However, some materials such as melamine–formaldehyde and urea–formaldehyde resins usually release poisonous formaldehyde in the application, which is hazardous to environment and health. In addition, many microencapsulated PCMs are easily flammable due to the chemical constitution of organic PCMs and organic polymer shell materials. So the microencapsulated PCMs with inorganic shell were also prepared in recent years.

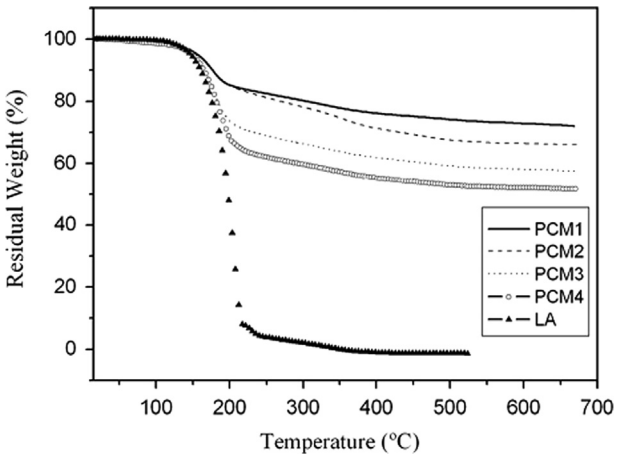


Fig. 6. TGA curves of the LA, and PCM1–PCM4 [42].

Table 1
Comparison of composite phase change materials with organic and inorganic supporting material.

PCMs/supporting material	Mass ratio	Melting		Solidifying	
		Temperature (°C)	Latent heat (kJ/kg)	Temperature (°C)	Latent heat (kJ/kg)
SA/PMMA [7]	80/20	67.31	187.72	66.78	190.34
PEG/cellulose [11]	80/20	57.18	152.16	44.76	138.39
DA/GGBS [16]	11/89	21.16	22.51	19.10	21.62
CA/HNT [19]	60/40	29.34	75.52	-	-
CA–MA/VMT [23]	20/80	19.75	17.05	27.46	31.42
Paraffin/GO [24]	48.3/51.7	53.57	63.76	44.59	64.89
LA/SiO_2 [27]	64.8/35.2	42.46	117.21	41.30	90.00
n-Hexadecane/SiO_2 [29]	73.3/26.7	20.08	147.58	16.07	145.10
SA/EG [31]	83/17	53.12	155.50	54.28	155.70
PA/active aluminum oxide [33]	47.4/52.6	56.86	78.79	60.25	84.48
PA/EG [35]	80/20	60.88	148.36	60.81	149.66
n-Octadecane/molecular sieve [36]	33.3/66.7	28.33	101.14	26.75	97.55
PEG/diatomite [37]	50/50	27.70	87.09	32.19	82.22
PA/SiO_2 [38]	41.1/58.9	59.76	85.11	59.20	60.55
CA–MA/EP [39]	55/45	21.70	85.40	20.70	89.75
LA/activated carbon [42]	33.3/66.7	44.07	65.14	42.83	62.96

3.1. Microencapsulated phase change materials with organic shell

The polymethylmetracrylate (PMMA) microcapsules containing n-octacosane as PCM for thermal energy storage were prepared by using a miniemulsion apparatus. The SEM results in Fig. 7 show that the PMMA/n-octacosane microcapsules have spherical shape with a fairly uniform structure and compact surfaces. The FT-IR results indicated that the PMMA shell microcapsules were successfully synthesized by emulsion polymerization. The DSC results revealed that the temperatures and latent heats of melting and freezing of the PMMA/n-octacosane microcapsule are 50.6 °C and 53.2 °C, 86.4 kJ/kg and 88.5 kJ/kg, respectively. The TGA analysis indicated that the microencapsulated n-octacosane degraded in two steps and had good chemical stability. The average latent heats of melting and freezing of the microencapsulated PCM after repeated 5000 thermal cycling were determined to be 79.9 kJ/kg and 81.7 kJ/kg, respectively. These results indicated that PMMA/n-octacosane microcapsules are reliable according to the thermal cycling tests [43].

The polyurea/polyurethane microcapsules with butyl stearate and paraffin as binary core materials were successfully synthesized via interfacial polymerization method. The phase change temperature of these microencapsulated PCMs (micro-PCMs) can be adjusted by regulating the composition of the binary core. The SEM photographs showed that these micro-PCMs have relatively spherical profiles and compact surfaces with diameter ranging from 5 to 15 μm. The DSC results indicated that the binary core content in micro-PCMs is in a range of 45–60 wt%. Moreover, after being treated under 50 °C for 7 days or subjected to thermal-cycling test for 500 times, the micro-PCMs have good thermal performances and stabilities. The TGA analysis demonstrated that the decomposition temperature of the micro-PCMs increases with the increasing dosage of butyl stearate and the molecular weight of the water-soluble monomers [44].

The p(n-butyl methacrylate-co-methacrylic acid) shell (P(BMA-co-MAA)) microcapsules containing n-alkane as PCMs for thermal energy storage were prepared by a suspension-like polymerization. The FTIR results confirmed that n-octadecane or paraffin wax was microencapsulated by the P (BMA-co-MAA) shell successfully. The DSC results indicated that the microcapsules containing n-octadecane or a paraffin wax have high phase change enthalpies of melting (130.3 kJ/kg or 123.9 kJ/kg) and freezing (125.8 kJ/kg or 118.4 kJ/kg). The TGA results revealed that the weight loss temperatures of the P(BMA-co-MAA)/n-alkane microcapsules are significantly increased as compared with the raw PCMs. The test results

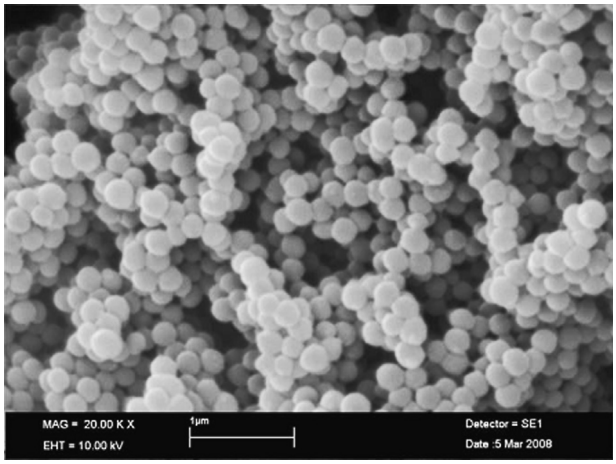


Fig. 7. SEM photograph of the PMMA/n-octacosane microcapsules [43].

indicated that the phase change enthalpies of the P(BMA-co-MAA)/n-alkane microcapsules changed little after thermal cycles [45].

Microencapsulated paraffin was synthesized by a complex coacervation method using gelatin and acacia as shell materials and paraffin as core material in an emulsion system. The experimental results indicated that a core/shell mass ratio of 2.0 was chosen for the preparation of microencapsulated paraffin. The SEM image showed that the microencapsulated paraffin was coated well. The particle size of the microencapsulated paraffin was about 81 μm. The DSC results indicated that the melting temperature of the microencapsulated paraffin is 52.05 °C, the melting latent heat is 141.03 kJ/kg, the solidification temperature is 59.68 °C, and the solidification latent heat is 121.59 kJ/kg. These results revealed that the microencapsulated paraffin for thermal energy storage has a larger phase change latent heat, suitable phase change temperature, and better thermal stability, therefore, it has a great potential to be used in thermal energy storage systems [46].

Microcapsules containing n-octadecane with crosslinked p(butyl methacrylate) (PBMA) and p(butyl acrylate) (PBA) shells were prepared by a suspension-like polymerization. Divinylbenzene (DVB) and pentaerythritol triacrylate (PETA) were employed as crosslinking agents. The microencapsulated PCMs (micro-PCMs) particles have a spherical profile with average diameter of 15 μm, 12 μm, 2 μm and 4 μm for micro-PCMs with BA–PETA, BMA–PETA, BA–DVB and BMA–DVB, respectively. The micro-PCMs prepared by using DVB presented greater heat capacities as compared with the

micro-PCMs prepared by using PETA. The melting and crystallization latent heats of the micro-PCM with 55.6% BMA–DVB are 126.4 kJ/kg and 123.7 kJ/kg. The thermal resistant temperatures of the microPCMs prepared by using DVB as crosslinking agent are higher than those of the microPCMs prepared by using PETA as crosslinking agent. The phase change temperatures and latent heats of the microcapsules changed little after 1000 thermal cycles [47].

The nanocapsules of a paraffin type PCM (RT80) with a melting temperature of 80 °C, in a styrene–butyl acrylate copolymer shell were prepared by miniemulsion polymerization. The encapsulation efficiency was determined to be 80 wt% with a particle size distribution between 52 nm and 112 nm and regular spherical shape and uniform structure. The amount of encapsulated paraffin was comprised between 8% and 20%. The DSC results indicated that the melting and crystallization heats are approximately 5–25 kJ/kg, mainly depending on surfactant/paraffin mass ratio. The melting temperature of RT80 nanoparticles slightly is decreased by 1–7 °C as compared to that of the raw RT80. In addition, the encapsulated RT80 nanoparticles showed good thermal stability even after 200 heating and cooling cycles [48].

Polyurea microcapsules containing PCMs were prepared successfully by using the interfacial polycondensation. Toluene-2,4-diisocyanate (TDI) and ethylenediamine (EDA) were chosen as monomers. Butyl stearate was used as a core material. The optical microphotographs of the microencapsulated PCMs showed the sizes of microcapsules are about 20–35 μm. The DSC results indicated that the phase change temperature of the microencapsulated PCMs is about 29 °C, and the latent heat of fusion is about 80 kJ/kg. After 400 heating and cooling cycles, the phase change temperature and the phase change enthalpy of encapsulated butyl stearate kept nearly the same value. The microencapsulated PCMs have a good thermal stability [49].

The microcapsulated PCMs were prepared by coating n-eicosane with polymethylmethacrylate (PMMA) shell. The particle size distribution (PSD) analysis revealed that the average diameter of the microcapsules is 0.70 μm under the stirring speed of 2000 rpm. The DSC results indicated that the melting and freezing temperatures and the latent heats of the microcapsules are 35.2 °C and 34.9 °C, 84.2 kJ/kg and 87.5 kJ/kg, respectively. The DSC results also showed that the PMMA microcapsules consisted of an average of 35 wt% eicosane. The thermal cycling tests presented that the PMMA/eicosane microcapsules are reliable. The TGA analysis showed that the PMMA/eicosane microcapsules degraded in three steps at considerably high temperatures [50].

The stearic acid/polycarbonate (SA/PC) microcapsule as a PCM for thermal energy storage was prepared by the solution casting method. The test results indicated that the SA was encapsulated successfully with the maximum mass fraction of 52% without leakage from the SA/PC microcapsule. The average diameter of the microcapsule is 0.50 μm. In the SA/PC microcapsule, two components (SA and PC) had good compatibility and no chemical reactions occurred between each other. The DSC results indicated that the melting and freezing temperatures and the latent heats of the microcapsule are 60.0 °C and 51.2 °C, 91.4 kJ/kg and 96.8 kJ/kg, respectively. Iron filings were used to improve thermal storage and release rates, and the rates were increased by 23% compared with the microcapsule without iron filings. The thermal cycling test revealed that the microcapsules have good thermal reliability after 1000 thermal cycles [51].

The polymethylmethacrylate (PMMA)/n-heptadecane microcapsules were prepared by emulsion polymerization technique at the emulsion stirring rate of 2000 rpm. The FT-IR results indicated that the n-heptadecane was successfully encapsulated inside the PMMA microcapsules. The SEM and PSD analyses revealed that the microcapsules had smooth, compact surface and spherical shape with average diameter of 0.26 μm. The DSC results showed that the temperatures of melting and freezing and latent heats of melting and freezing of the PMMA/n-heptadecane microcapsules are 18.2 °C and 18.4 °C and 81.5 kJ/kg and 84.2 kJ/kg, respectively. The microencapsulation ratio of the n-heptadecane in the PMMA microcapsules was determined to be 38 wt%. The TGA analysis presented that the PMMA/n-heptadecane microcapsules degraded in three steps and resisted to high temperatures. The thermal cycling test showed that the microcapsules have good thermal reliability and chemical stability after 5000 melting and freezing cycles [52].

The microcapsules containing n-octadecane with different methylmethacrylate (MMA)-based copolymer shells were prepared by a suspension-like polymerization. Butyl acrylate (BA), butyl methacrylate (BMA), lauryl methacrylate (LMA) and stearyl methacrylate (SMA) were used as monomers to copolymerize with MMA. Pentaerythritol tetraacrylate (PETRA) was employed as a crosslinking agent. The DSC results showed that the melting and crystallization enthalpies of the microcapsules are 173.7 kJ/kg and 174.4 kJ/kg as the n-octadecane content is 77.3% in the crosslinked microencapsulted PCMs with P(MMA-co-BMA) shell. The heat capacities of the crosslinked microencapsulted PCMs were higher than those of their uncrosslinked counterparts. The crosslinked microencapsulted PCMs exhibited significantly better thermal stabilities compared with their uncrosslinked counterparts and the n-ontadecane bulk. The crosslinked microencapsulted PCMs with P(MMA-co-SMA) presented the highest thermal resistance temperature up to 255 °C [53].

The polymethylmethacrylate (PMMA) microcapsules containing docosane were prepared by emulsion polymerization. The SEM and PSD analyses showed that the microcapsules had smooth and compact surface with average diameter of 0.16 μm. The DSC results indicated that the docosane in the microcapsules melts at 41.0 °C and crystallizes at 40.6 °C, and the latent heats of melting and crystallization are 54.6 kJ/kg and 48.7 kJ/kg, respectively. The test results also showed that the microcapsule consisted of an average of 28 wt% docosane. The TGA investigation revealed that the PMMA/docosane microcapsules degraded in three steps and had good chemical stability [54].

The nanocapsules used as PCM were prepared by using in situ polymerization methods. The n-tetradecane was used as the core material. Urea and formaldehyde were used for the shell polymerization. Sodium dodecyl sulfate was used as the emulsifier and resorcin was used as the system modifier. Fig. 8 shows the DSC curves of nanocapsules. The DSC results indicated that the fusion latent heat of the nanocapsules is 134.16 kJ/kg as the mass content of the n-tetradecane is up to 60%. It is observed that the pure ntetradecane has a supercooling degree of 3.29 °C, the supercooling degrees of the nanocapsules are all below 3 °C. It can be concluded that the encapsulation of the n-tetradecane could slightly decrease the supercooling degree of the PCM due to shell of the nanocapsule could be used as crystal nucleus of the PCM. The TGA revealed that the thermal stability of the nanocapsules can be improved by the NaCl additive in the polymerization. It is found that the 2–5% NaCl concentration is suitable for the n-tetradecane encapsulation, and n-tetradecane can be encapsulated efficiently with good thermal stability. The nanocapsules can be applied for thermal energy storage and heat transfer enhancement [55].

The modified polymethylmethacrylate (PMMA) microcapsules containing a hydrated salt $Na_2HPO_4 \cdot 7H_2O$ were prepared by means of the suspension copolymerization-solvent volatile method. The formation of the microcapsules with the PMMA shell was confirmed during emulsion polymerization by FT-IR spectra results. The $Na_2HPO_4 \cdot 7H_2O$, from the dehydration of precursor $Na_2HPO_4 \cdot 12H_2O$, was determined to be the core PCM encapsulated in the microencapsulated PCMs. The microcapsules had smooth and compact surface with spherical shape of mean diameter about 6.8 μm. The TGA

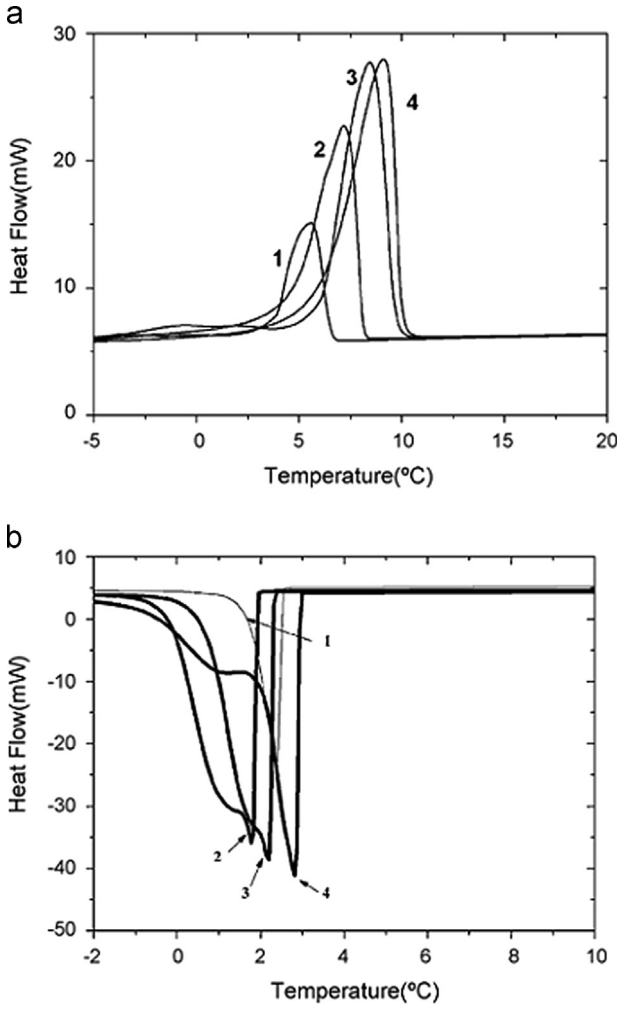


Fig. 8. DSC curves of the nanocapsules with (1) 0.25%, (2) 1%, (3) 2% and (4) 5% resorcin concentration used as system modifier in the preparation (a) the heating process and (b) the cooling process [55].

results showed that the weight loss of the PMMA/$Na_2HPO_4 \cdot 7H_2O$ microencapsulated PCMs was less than 10% in the temperature range from 30 °C to 84 °C. The DSC results indicated that the melting temperature and fusion latent heat of the microencapsulated PCMs are about 51 °C and 150 kJ/kg. The encapsulation of the microcapsules played a very significant role to reduce the supercooling degree of the inorganic hydrated salt. The PMMA/$Na_2HPO_4 \cdot 7H_2O$ microencapsulated PCMs have promising potentials in thermal storage applications [56].

3.2. *Microencapsulated phase change materials with inorganic shell*

The microencapsulated PCM based on an n-octadecane core and an inorganic silica shell was synthesized by using tetraethyl orthosilicate (TEOS) as an inorganic source through a sol–gel process. The FTIR spectra indicated that the n-octadecane was successfully encapsulated within the silica shell material. These silica microcapsules presented a spherical morphology with a well-defined core–shell microstructure and a large particle size distributed in the range of 7–16 μm. The n-octadecane inside the silica microcapsules still retained a good crystalline. The TGA results showed that the silica microcapsules degraded in two separate steps and have good thermal stability. The silica-microencapsulated n-octadecane has a smooth and compact shell structure, and thus has good phase-change performance and high encapsulation efficiency by controlling the loading of core material and acidity of the reaction solution during the sol–gel process. The thermal conductivity of the microencapsulated n-octadecane was also significantly improved due to the presence of the high thermal conductive silica shell [57].

The microencapsulated stearic acid (SA) with silicon dioxide (SiO_2) shell as composite thermal energy storage material was prepared using sol–gel methods. In the composite thermal energy storage material, the SA was used as the core material, and the SiO_2 acted as the shell material which prevented the leakage of the melted SA. Fig. 9 shows the DSC curves of the SA, MPCM1–MPCM3. The DSC results indicated that the microencapsulated SA with the SiO_2 shell solidifies at 52.6 °C with a latent heat of 162.0 kJ/kg and melts at 53.5 °C with a latent heat of 171.0 kJ/kg when the encapsulation ratio of the SA is 90.7%. It is found that the encapsulation ratios of the MPCM1–MPCM3 are 89.2%, 89.8% and 90.6%, correspondingly. The higher SA content, the higher encapsulation ratio of the MPCM. The TGA results presented that there are two-step thermal degradation processes: the first step takes place at the temperature between 150 and 300 °C, corresponding to the thermal degradation of the SA molecular chains. The second step occurs from 350 to 500 °C, representing to the thermal degradation of the SiO_2 molecular. The SiO_2 shells are advantageous to form carbonaceous-silicate charred layer building up on the surface, which insulates the core material and slows the escape of the volatile products generated during thermal degradation. Therefore, the SiO_2 shells can improve

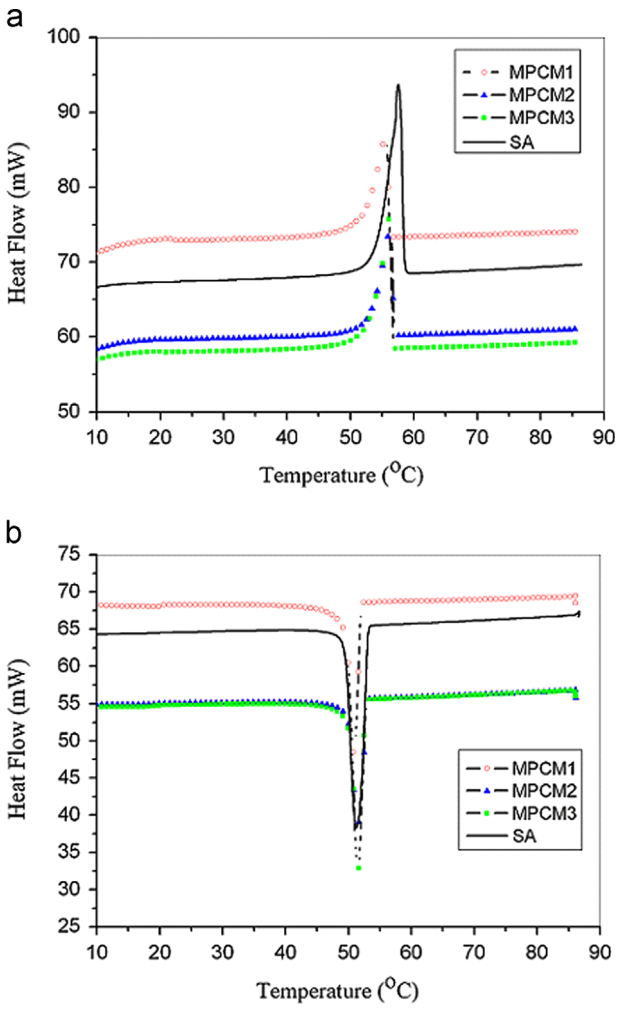


Fig. 9. DSC curves of the SA, MPCM1, MPCM2 and MPCM3 (a) the melting process and (b) the solidifying process [58].

the thermal stability of the microencapsulated SA as composite thermal energy storage material [58].

The microencapsulated palmitic acid (PA)/AlOOH was prepared using an in situ emulsion interfacial poly-condensation method. The resulting colloidal–sphere microcapsules are of core–shell microstructures with diameter around 200 nm. The DSC results indicated that melting temperatures of the microencapsulated PCMs for the samples P1–P3 are 12.7 °C, 13.8 °C and 16.0 °C, respectively, and their melting latent heats are 19.0 kJ/kg, 22.6 kJ/kg and 27.8 kJ/kg, respectively. This means that their melting temperatures are decreased significantly relative to that of the pristine PA, which might originate from the strong interface interactions between the core and shell in the PA/AlOOH microcapsules. The thermal storage capabilities for the microcapsules P1–P3 are 19.6%, 21.2% and 21.6%, respectively [59].

The microencapsulated PCMs (micro-PCMs) based on n-octadecane core and silica shells were synthesized through interfacial polycondensation in different conditions. It is known that the microcapsules formed at pH 2.89 obtained a compact silica shell with fairly smooth surface as well as a large mean particle size of about 17.0 μm. The TGA results indicated that the silica microcapsules have a typical two-step degradation process and presented a good thermal stability. The DSC results showed that the silica-microencapsulated n-octadecane can achieve good phase change properties and high encapsulation efficiency by controlling the acidity of the reaction solution as well as the loading content of core material. The thermal conductivity of the silica microcapsules was also significantly improved due to the presence of high thermal conductive silica shell. The sample synthesized with the n-octadecane/tetraethyl orthosilicate (TEOS) weight ratio of 50/50 attained a high thermal conductivity of 0.6547 W/m K due to its thick shell [60].

The microencapsulated paraffin composites with SiO_2 shell as thermal energy storage materials were prepared using sol–gel methods. In the microencapsulated composites, paraffin was used as the core material that is a PCM, and SiO_2 acted as the shell material that is fire resistant. The DSC results indicated that the microencapsulated paraffin composites solidify at 58.27 °C with a latent heat of 107.05 kJ/kg and melt at 58.37 °C with a latent heat of 165.68 kJ/kg when the encapsulation ratio of the paraffin is 87.5%. It is also found that the difference between solidifying onset temperature and peak temperature of the MEPCM1, MEPCM2 and MEPCM3 is smaller than that of the paraffin. This indicates the supercooling degree of the MEPCM1–MEPCM3 is smaller than that of the paraffin during solidification process due to interior wall of the SiO_2 shells acts as nucleation agent. The TGA curves of the MEPCM1–MEPCM3 are shown in Fig. 10. It can be observed from Fig. 10 that there are two-step thermal degradation processes: the first step takes place at the temperature between 20 and 80 °C, corresponding to the release of water molecules adsorbed in the shells of the SiO_2, and the second step occurs from 200 to 350 °C, corresponding to the thermal degradation of the paraffin molecular chains. The weight loss of the MEPCM3 is relatively larger than that of the MEPCM1 and MEPCM2 during two-step thermal degradation processes. The TGA results showed that the SiO_2 shells can improve the thermal stability of the microencapsulated paraffin composites due to the synergistic effect between the paraffin and SiO_2 [61].

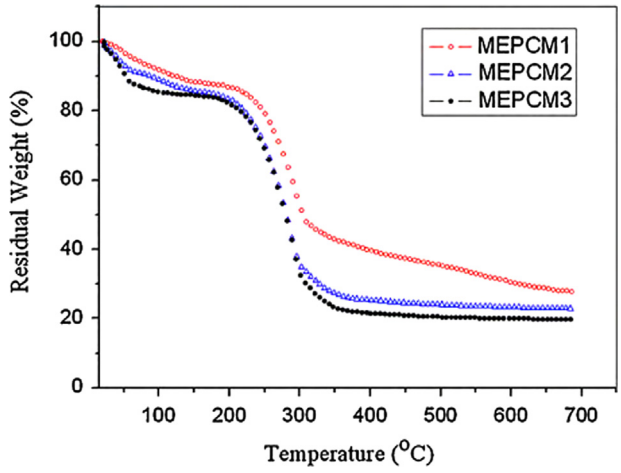


Fig. 10. TGA curves of the MEPCM1–MEPCM3 [61].

3.3. Comparison of microencapsulated phase change materials with organic and inorganic shell

Microencapsulated PCMs can be prepared by physical and chemical methods, such as spray-drying, complex coacervation, interfacial polycondensation, in-situ polymerization, and so on. The manufacturing efficiency of the microencapsulated PCMs is influenced by synthesis methods and preparation parameters, such as core/shell mass ratio, temperature and pressure of the preparation process, pH value of the solution, stirring speed, etc. Table 2 shows the comparison of microencapsulated phase change materials with organic and inorganic shell. It is found that the stearic acid/SiO_2, n-octadecane/methylmethacrylate and paraffin/SiO_2 microencapsulated PCMs have the higher encapsulation ratio, and latent heats of these microencapsulated PCMs are higher accordingly. The results also indicate that the docosane/PMMA, n-eicosane/PMMA and n-heptadecane/PMMA microencapsulated PCMs have the lower encapsulation ratio, and latent heats of these microencapsulated PCMs are smaller accordingly. It is concluded that the SiO_2 and methylmethacrylate are better as shell material of microencapsulated PCMs than PMMA shell.

Table 2
Comparison of microencapsulated phase change materials with organic and inorganic shell.

Core/shell	Encapsulation ratio (%)	Melting		Solidifying	
		Temperature (°C)	Latent heat (kJ/kg)	Temperature (°C)	Latent heat (kJ/kg)
n-Octacosane/PMMA [43]	–	50.6	86.4	53.2	88.5
Paraffin/gelatin and acacia [46]	66.7	52.1	141.0	59.7	121.6
Butyl stearate/polyurea [49]	–	29.0	80	–	–
n-Eicosane/PMMA [50]	35	35.2	84.2	34.9	87.5
Stearic acid/polycarbonate [51]	52	60.0	91.4	51.2	96.8
n-Heptadecane/PMMA [52]	38	18.2	81.5	18.4	84.2
n-Octadecane/methylmethacrylate [53]	77.3	–	173.7	–	174.4
Docosane/PMMA [54]	28	41.0	54.6	40.6	48.7
Stearic acid/SiO_2 [58]	90.7	53.5	171.0	52.6	162.0
Paraffin/SiO_2 [61]	87.5	58.4	165.7	58.3	107.1

4. Various encapsulation techniques of the microencapsulated phase change materials

Microencapsulated PCMs are usually synthesized by using following encapsulation techniques: in situ polymerization, interfacial polymerization, suspension polymerization, sol–gel process, complex coacervation and spray drying. Physical methods such as spray drying or fluidized bed cannot regulate the sizes of the microcapsules, and the diameters of the microcapsules are larger than 100 μm. The chemical methods such as in situ polymerization, interfacial polymerization, suspension polymerization, sol–gel process and complex coacervation may be restricted by the high cost of preparation process and the use of organic solvents, which brings the environmental and health problem during the polymerization process.

4.1. *In situ polymerization*

The microencapsulated phase change materials (micro-PCMs) with adjustable phase change temperature were prepared by the in situ polymerization method. The butyl stearate and paraffin were used as binary core materials, and poly (methyl methacrylate-co-divinylbenzene) (P(MMA-co-DVB)) copolymer acted as shell material. The phase change temperature of the micro-PCMs can be adjusted by regulating the weight ratio of butyl stearate to paraffin. As shown in Fig. 11, the micro-PCMs possessed relatively spherical profiles and compact surfaces with diameter ranging from 5 to 10 μm [62].

The micro-PCMs with melamine–formaldehyde (MMF) as the shell and paraffin as the core were synthesized by the in situ polymerization. A series of the micro-PCMs samples were fabricated under emulsion stirring rates in range of 1000–3000 rpm with core/shell weight ratios of 3/1, 2/1, 1/1, 1/2 and 1/3. Fig. 12 shows the SEM photograph of the micro-PCMs containing paraffin. It can be observed that the micro-PCMs have regular spherical shape with smooth surface, and its average diameter is about 20 μm. The DSC results indicated that the shell of the micro-PCMs had not influence on the phase change properties of pure paraffin [63].

The micro-PCMs with n-octadecane core and resorcinol-modified melamine–formaldehyde shell were prepared by the in situ polymerization method. The SEM results showed that the microcapsules with a core/shell weight ratio of 75/25 have a compact surface of the shell and a mean particle size is below 20 μm. The DSC results indicated that the micro-PCM under this condition has much better phase change properties than the others and the efficiency of encapsulation is about 92%. The anti-osmosis measurement result also showed that the micro-PCM has a better stability [64].

The microcapsules with n-hexadecane core and melamine–formaldehyde shell were synthesized via an in situ polymerization process. The n-hexadecane was added into an aqueous solution of melamine–formaldehyde pre-polymer and surfactant. This mixture was vigorously dispersed by a homogenizer. The emulsion was regulated to 4 of pH value by 10 wt% citric acid solution. Polymerization of melamine–formaldehyde and microencapsulation were achieved with continuous agitation for 4 h at 55 °C. Then, the pH value of the solution was regulated to 9 with 50 wt% triethanolamine solution to complete the reaction. The tensiometric measurements indicated that the optimum emulsion conditions were attained with a binary mixture of Tween-20 and Brij-35, a phase volume ratio of 0.42 and a pH value regulated to 4. The microcapsules with a mean diameter between 0.5 and 10 μm could be obtained by adjusting the stirring rate and stirring time [65].

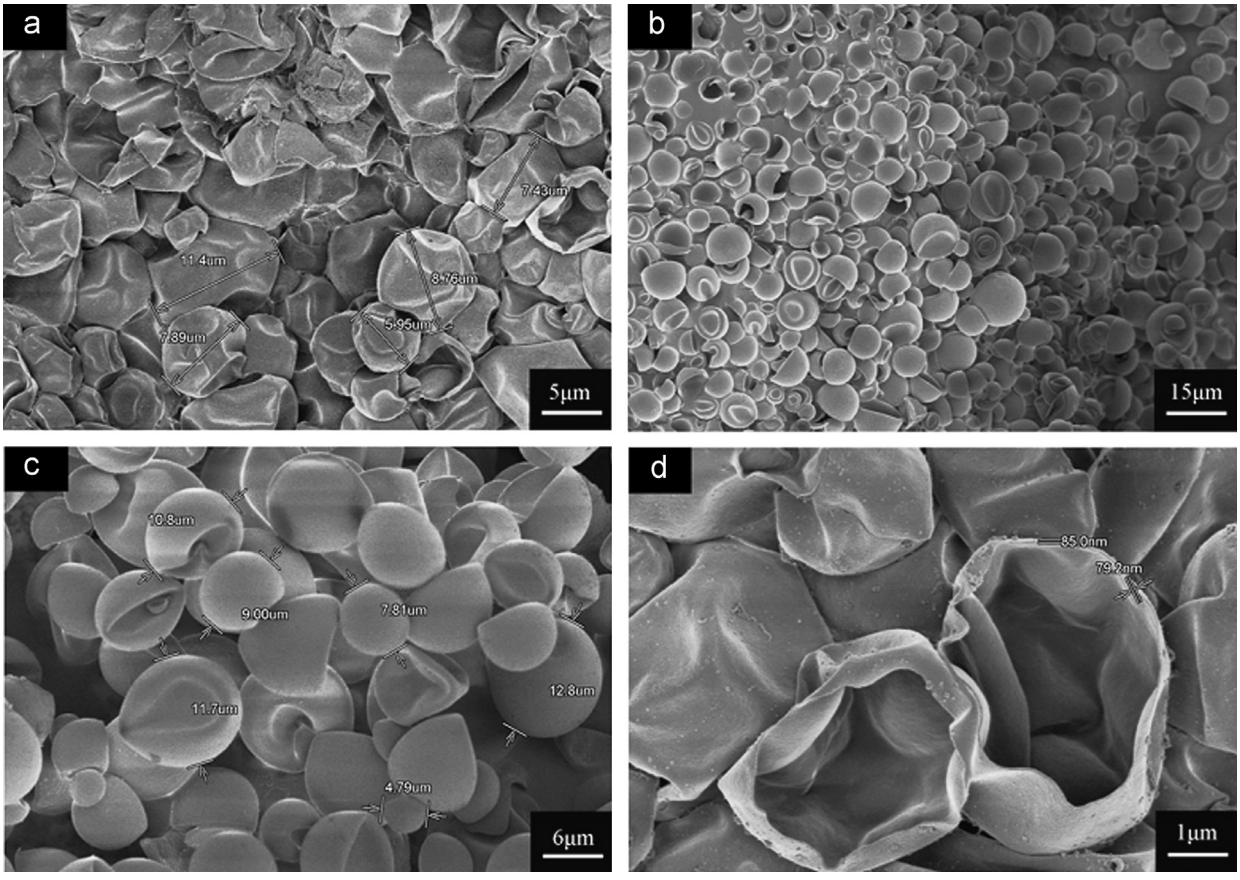


Fig. 11. SEM photographs of the micro-PCMs with the weight ratio of paraffin to butyl stearate is 4.5:0.5 (a) sample 1, (b) sample 2, (c) sample 3, and (d) the broken shell of sample 1 [62].

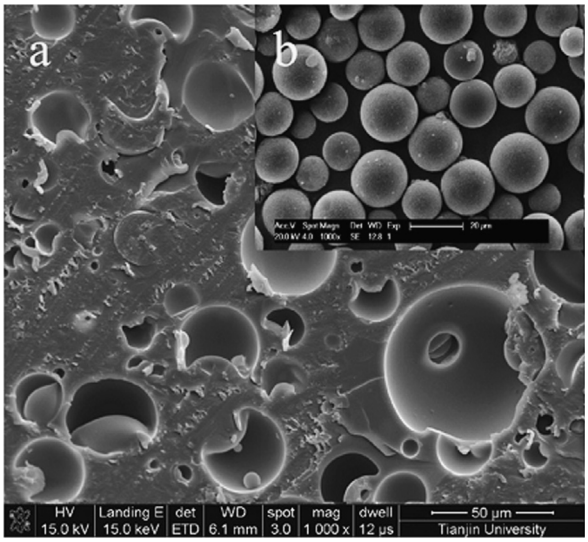


Fig. 12. SEM photograph of the microPCMs containing paraffin [63].

4.2. Interfacial polymerization

The micro-PCMs with butyl stearate core and polyurea shell were prepared by interfacial polycondensation. Toluene-2,4-diisocyanate (TDI) and ethylenediamine (EDA) were chosen as monomers. The butyl stearate was dissolved in an organic solution comprising cyclohexane and TDI (oil soluble monomers), and an aqueous solution of OP-10 was prepared. Then the organic solution was added to the aqueous surfactant solution and the mixture was emulsified mechanically at a stirring rate of 500 rpm/min to obtain an O/W emulsion. After stirring for few minutes, the aqueous soluble monomers (EDA) were added into the emulsion system and the mixture was heated to 65 °C. The interfacial polycondensation reaction occurred between TDI and EDA at the oil–water interface for about 2–3 h. The results indicated that the phase change temperature of the micro-PCMs is about 29 °C and the latent heat of fusion is about 80 kJ/kg. The optical microphotograph showed that the particle diameter is 20–35 µm [49].

The microcapsules were synthesized by interfacial polycondensation with toluene-2,4-diisocyanate (TDI) and diethylenetriamine (DETA) as monomers. Octadecane was used as a PCM and NP-10 was used as an emulsifier. The polyurea microcapsules were formed not only by reaction with TDI and DETA, but also by reaction of TDI with hydrolyzed at the interface. The TDI was reacted with DETA in the weight ratio of 3:1, and the NP-10 was reacted with TDI to form urethane. The results indicated that the phase change temperature of the microcapsules is at 29–30 °C. The encapsulation efficiency of the octadecane increased as the core content decreased. The SEM results showed that the microcapsules have regular spherical shape with smooth surface, and its average diameter is about 1 µm [66].

4.3. Suspension polymerization

The micro-PCMs with paraffin wax core were prepared through a suspension polymerization using a copolymer of methyl methacrylate (MMA) and styrene (St) as shell. The synthesis process included two phases: a continuous phase containing water and polyvinylpyrrolidone, and a discontinuous phase containing styrene, methyl methacrylate, paraffin wax and benzoyl peroxide. The continuous phase was transferred to the glass reactor with mild agitation (150 rpm). The initiator was premixed with monomers and phase change material. The discontinuous phase was then added to the continuous phase and was kept under vigorous agitation (500 rpm) at a constant temperature of 98 °C. The polymerization process was performed for 5 h under a nitrogen atmosphere. It is found that as the amount of MMA was increased, the reaction time and the mean particle size decreased, and the paraffin was not encapsulated when the monomers/paraffin mass ratio was lower than 3.0 due to the shortage of copolymer. The experimental results indicated that the MMA/St mass ratio of 4.0 and monomers/paraffin ratio of 3.0 are the best conditions to synthesize the microcapsules [67].

The micro-PCMs with n-octadecane core were synthesized by suspension polymerization using different crosslinked methylmethacrylate-based polymer as shells. The 1,4-butylene glycol diacrylate (BDDA), divinylbenzene (DVB), trimethylolpropanetriacrylate (TMPTA) and pentaerythritol tetraacrylate (PETRA) were used as crosslinking agents. The reaction substances involved two phases: a continuous phase containing water and styrene-maleic anhydride polymer (SMA), and a discontinuous phase containing methylmethacrylate (MMA), crosslinking agent, n-octadecane and initiator. The continuous phase was transferred to the glass reactor with mild agitation. The initiator was premixed with MMA, crosslinking agent and n-octadecane. Then, the discontinuous phase was added into the continuous phase and was kept for 15 min under vigorous agitation (1000 rpm) at a constant temperature of 35 °C to obtain a stable oil-in-water emulsion. The polymerization process was carried out under vigorous agitation (540 rpm) at a constant temperature of 85 °C. The test results indicated that the micro-PCMs containing 75.3 wt% n-octadecane using PETRA as crosslinking agent have the highest melting latent heat of 156.4 kJ/kg and crystallization heat of 182.8 kJ/kg, and display the best thermal stability and shell mechanical strength. It is found that the micro-PCMs with DVB have a relatively higher shell mechanical strength and heat capacity compared with those prepared with BDDA [68].

4.4. Sol–gel polymerization

The nanocapsules containing palmitic acid (PA) as core and SiO_2 as shell materials were synthesized through the sol–gel polymerization by changing the value of pH in the range of 11–12. The sodium dodecylsulfate (SDS) was dissolved in the distilled water at 70 °C, then the PA was added into this solution which was stirred continuously with a magnetic stirrer at the rate of 1000 rpm for 2 h to form the PA emulsion. The tetraethoxysilane (TEOS) and absolute ethanol were mixed with distilled water and the pH of the solvent was regulated by adding ammonium hydroxide. The mixture was stirred with a magnetic stirrer at the rate of 500 rpm for 30 min. The pH of the solvent was adjusted at 11(S1), 11.5(S2) and 12(S3) in three different beakers. When the hydrolysis reaction of the silica was completed, the resultant sol solution was used as the encapsulation precursor. The sol solution was added drop wise into the PA emulsion which was stirred at the rate of 500 rpm for 4 h. The temperature of the emulsion was maintained at 70 °C. Then the emulsion was cooled to room temperature and washed with distilled water. The SEM results showed that the nanocapsules have regular and spherical shape with an average diameter size of 183.7, 466.4 and 722.5 nm for pH values 11, 11.5 and 12, respectively. The DSC results indicated that the melting latent heat was increased to 180.91 kJ/kg and solidifying latent heat was increased to 181.22 kJ/kg at high pH value. The encapsulation ratios were increased from 83.25% at 11 of pH value to 89.55% at 12 of pH value [69].

The microencapsulated paraffin with TiO_2 shells as shape-stabilized thermal energy storage materials were prepared through a sol–gel polymerization. The paraffin and SDS in different mass ratio were added into deionized water to form an oil/water (O/W) emulsion in a beaker. Then the solution was continuously stirred at a rate of 800 rpm for 40 min with a magnetic stirrer

Table 3
The advantages and disadvantages of various encapsulation techniques.

Encapsulation techniques	Advantages	Disadvantages
In situ polymerization	• Small size of the microcapsules. • Uniform distribution of the microcapsules. • Tight shell of the microcapsules. • Good stability of the microcapsules.	• Reasonable mass ratio of the monomer. • Temperature control of the reaction. • pH value regulation of the reaction. • Use of formaldehyde.
Interfacial polymerization	• Small size of the microcapsules. • Uniform distribution of the microcapsules. • Tight shell of the microcapsules. • Good stability of the microcapsules.	• Reasonable mass ratio of the monomer. • Temperature control of the reaction. • Suitable emulsor.
Suspension polymerization	• Small size of the microcapsules. • Uniform distribution of the microcapsules. • Tight shell of the microcapsules. • Good stability of the microcapsules.	• Reasonable mass ratio of the monomer. • Temperature control of the reaction. • Suitable emulsor.
Sol–gel polymerization	• Small size of the microcapsules. • Uniform distribution of the microcapsules. • Tight shell of the microcapsules. • Good stability of the microcapsules.	• Reasonable mass ratio of the monomer. • pH value regulation of the reaction.
Complex coacervation	• pH value regulation of the reaction. • Temperature control of the reaction.	• Big size of the microcapsules. • Loose shell of the microcapsules. • Poor stability of the microcapsules.
Spray drying	• Temperature control of the reaction. • Spray speed control.	• Big size of the microcapsules. • Nonuniform distribution of the microcapsules. • Loose shell of the microcapsules. • Poor stability of the microcapsules.

while the temperature was controlled at 70 °C. Finally, the paraffin was dispersed uniformly in the O/W microemulsion, and the pH value was adjusted to 2–3 using hydrochloric acid. The tetra-n-butyl titanate (TNBT) and anhydrous ethanol in different mass ratio were mixed in another beaker to form the solution. The solution was added into the paraffin microemulsion drop by drop, while the stirring rate was kept at 800 rpm and the temperature was controlled at 70 °C using a constant temperature bath for 1 h. The DSC and TGA results indicated that the microencapsulated paraffin melts at 58.8 °C with a latent heat of 161.1 kJ/kg and solidifies at 56.5 °C with a latent heat of 144.6 kJ/kg as the microencapsulation ratio is 85.5%, and the onset degradation temperature of the paraffin in the microcapsules is beyond 200 °C while the working temperature of the microcapsules is usually within 40–80 °C [70].

4.5. Complex coacervation

The microcapsules using caprylic acid as core with different wall materials, including urea–formaldehyde resin, melamineformaldehyde resin, ureamelamine–formaldehyde resin were prepared by using the coacervation method. Hardening process of microencapsulated PCMs was performed with formaldehyde. Prior to encapsulation core material, the caprylic acid was dispersed into a first monomer of shell solution with emulsifier. After 30 min the second monomer of shell solution was added to the prepared dispersion. The mixture was emulsified mechanically for 2–3 h at a stirring rate 1000 rpm. The next steps were addition of acid solution for adjusting the pH value, and addition of water for dilution of the emulsion solution. Finally, the microcapsules were stabilized by formaldehyde acted as crosslinking agent. The test results indicated that the phase change enthalpies of melting and freezing are 93.9 kJ/kg and 106.1 kJ/kg, respectively, and the particle diameter is 200 nm–1.5 μm [71].

Microcapsules of coco fatty acid mixture were prepared using the complex coacervation method. The core material was firstly dispersed in an aqueous 10% by weight gelatin solution at a temperature range of 40–60 °C, at which the wall material solution (urea, melamine, b-naphthol, gelatin) is liquid. Only in complex coacervation technique, gum Arabic, a polyanion or negatively charged polymer was added to the gelatin solution. The process was followed by adjusting the pH value and concentration of polymer so that a liquid complex coacervate formed. The pH value was typically between 4.0 and 4.5. Once the liquid coacervate was formed, the system was cooled to room temperature. Finally, hardening of microencapsulated PCMs was performed by using formaldehyde. After that, the pH value was increased to 9–11 by NaOH solution. The microcapsules were then cooled down to 5–10 °C and kept at this temperature for 2–4 h. The experimental results indicated that microcapsules have a spherical geometrical shape, and the microencapsulated PCM melts in the temperature range of 29–31 °C. It is found that the mixtures of the gelatin and gum Arabic are the best wall materials for microencapsulating coco fatty acid [72].

4.6. Spray drying

The microencapsulated paraffin Rubitherm RT27 with and without carbon nanofibers (CNFs) using polyethylene–EVA as a polymer shell was prepared through spray drying technique. A homogeneous liquid solution (feed stream) was atomized by means of a carrier gas stream (compressed N2). After atomization, the solvent was evaporated and the particles were dried by an additional nitrogen stream (drying N2) in the drying chamber.

The final product was recovered in the collector. The test results indicated that the thermal energy storage capacity of this microcapsule with 98.1 kJ/kg was similar to that of the microcapsule with 96.7 kJ/kg produced by a suspension polymerization technique using styrene as shell material [73].

4.7. Comparison of various encapsulation techniques

The advantages and disadvantages of various encapsulation techniques for the microencapsulated PCMs are presented in Table 3. It is found that the microcapsules with small size, uniform distribution, tight shell and good stability can be acquired by using in situ polymerization, interfacial polymerization, suspension polymerization and sol–gel polymerization methods. As shown in Table 3, the microcapsules with the big size, loose shell and poor stability are prepared by complex coacervation and spray drying techniques. In addition, in situ polymerization technique, the formaldehyde resins are usually used as shell materials for the protection of the PCMs, such as melamine–formaldehyde resins and urea–formaldehyde resins. The melamine–formaldehyde and urea–formaldehyde resins shell materials usually release poisonous formaldehyde in the application, which can cause environmental and health problems. Therefore, it is concluded that the interfacial polymerization, suspension polymerization and sol–gel polymerization methods can be utilized to synthesize the microencapsulated PCMs in various encapsulation techniques.

5. Applications of shape-stabilized thermal energy storage materials

The applications of shape-stabilized thermal energy storage materials in building energy conservation, air-conditioning systems, solar thermal application, thermal regulating textile materials, and some other practical latent heat thermal storage applications have been developed in recent decade. The shape-stabilized PCMs in building products can store significant amounts of thermal energy without large structural mass associated with sensible heat storage, which not only can reduce building energy consumption, but also flatten the fluctuation of indoor temperature and improve the indoor thermal environment and building performances.

5.1. Applications of composite phase change materials

The thermal performance of a hybrid space-cooling system with night ventilation and thermal storage using shape-stabilized PCM was investigated numerically. Natural cool energy was charged to the shape-stabilized PCM plates by night ventilation with air change per hour of 40 h^{-1} and was discharged to room environment during daytime. Additional cool-supply was provided by an active system during office hours (8:00–18:00) necessary to keep the maximum indoor air temperature below 28 °C. The results indicated that the thermal-storage effect of the shape-stabilized PCM plates combined with night ventilation could improve the indoor thermal-comfort level and save 76% of daytime cooling energy consumption (compared with the case without the shape-stabilized PCM and night ventilation) in summer in Beijing. Fig. 13 illustrates the daily variation of auxiliary cool-supply with and without shape-stabilized PCM plates under night ventilation and without night ventilation when the indoor temperature is kept in the desired range. It is found that when night ventilation is used, the daytime auxiliary cool-supply is much decreased due to the cool storage at night by the envelope. For most of summer days, the cool-supply for the case with shape-stabilized PCM plates is lower than that without shape-stabilized PCM plates, which represents the advantages of saving energy by

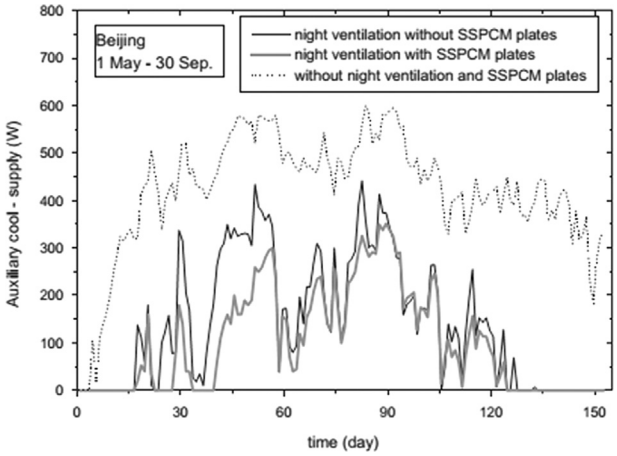


Fig. 13. Daily variation of auxiliary cool-supply with and without shape-stabilized PCM plates [74].

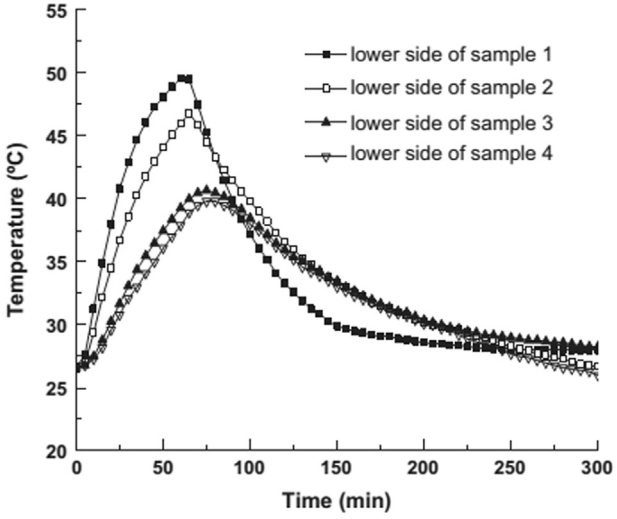


Fig. 14. The temperature change of the unheated surface of the wall samples 1–4 with the different heating time [75].

using shape-stabilized PCM thermal storage. The results also showed that the electrical coefficient of performance (COP) of night ventilation (the reduced cooling energy divided by fan power) was 7.5 and 6.5 for cases with and without the shape-stabilized PCM, respectively [74].

The thermal properties of the shape-stabilized PCM walls with different structure were investigated. The PCM is composed of paraffin mixture and high-density polyethylene. The walls including concrete and shape-stabilized PCM were prepared respectively by different methods, such as the direct mixing method and the lamination interpolation method. Heat transfer process in the shape-stabilized PCM walls was studied by comparing with traditional wall. Fig. 14 shows the temperature change of the unheated surface of the wall samples 1–4 with the different heating time. It can be seen that the increasing of the temperature of the unheated side of the wall is smaller than that of the common wall. From the temperature test results, we can know that (1) the effect of shape stabilized PCM wall 2 by direct mixing method is the worst, and the temperature reduction can reach most greatly to 4.4 °C; (2) the effect of shape stabilized PCM wall 4 is the best, and the temperature reduction can reach most greatly to 12.3 °C; and (3) the effect of phase stabilized PCM wall 3 is mediation, and the temperature reduction can reach most greatly to 10.8 °C. The results also indicate that the energy-saving effect of the shape-

stabilized PCM walls prepared by the lamination interpolation method was better than that of the shape stabilized PCM walls by direct mixing. There was no leakage for the shape stabilized PCM wall in the process of heating, which indicated that the PCM content of 70% in shape stabilized PCM is suitable [75].

The thermal performances of two PCM composites, mixed type PCM–gypsum and shape-stabilized PCM plates, were numerically investigated in a passive solar building in Beijing with an enthalpy model. The enthalpy model was applied for the simulation of shape-stabilized PCM wall. The schematic diagram of heat transfer through the exterior wall is shown in Fig. 15.

The transient enthalpy equation is [77]

$$\rho_j \frac{\partial H}{\partial \tau} = k_j \frac{\partial^2 t}{\partial x^2} \tag{1}$$

where for PCM composite, $H = \int_{t_0}^{t_1} c_{p,s}\, dt + \int_{t_1}^{t_2} c_{p,m}\, dt + \int_{t_2}^{t} c_{p,l}\, dt$; for the insulation layer and the hollow brick layer, $H = \int_{t_0}^{t} c_{p,j}\, dt$. The temperature range of phase transition is from t_1 to t_2.

The initial condition is

$$t(x,\tau)|_{\tau=0} = t_{init} \tag{2}$$

The boundary conditions for the surface exposed to the outside and inside air are

$$q_{r,out} + h_{out}(t_{out} - t_{i,out}) = -k_i \left.\frac{\partial t}{\partial x}\right|_{x=0} \tag{3}$$

$$q_{r,in} + h_{in}(t_{in} - t_{p,in}) = k_p \left.\frac{\partial t}{\partial x}\right|_{x=x_3} \tag{4}$$

For the exterior wall, $q_{r,in}$ and $q_{r,out}$ are indoor and outdoor radiation heat flux, respectively.

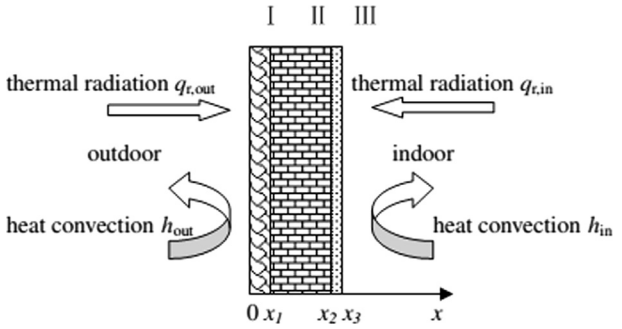


Fig. 15. Schematic diagram of heat transfer on the exterior wall surfaces (I – insulation layer, II – hollow brick, and III – PCM composite) [76].

The indoor temperature variation is illustrated in Fig. 16. The results showed that both mixed type PCM–gypsum and shape-stabilized PCM plates can effectively shave the indoor temperature swing by 46% and 56%, respectively. It is presented that although they both contain the same amount of PCM, the shape-stabilized PCM plates performs thermally better than the mixed type PCM–gypsum due to the smaller thermal resistance and relatively larger energy storage capacity per unit thickness. This implies that the shape-stabilized PCM plates responded more rapidly than the mixed type PCM–gypsum [76].

In order to protect the spacecraft attacked by the high energy, a new guard method was proposed. The shape-stabilized PCM with high thermal conductivity was used on the spacecraft. To prove the feasibility of using the material on spacecraft attacked by high energy, the thermal responses for spacecraft with shape-stabilized PCM were investigated in situations of normal and short-term high heat flux, in contrast to that with conventional thermal control system. The temperature of the PCM in different thermal conductivity is shown in Fig. 17. As thermal conductivity is 0.29, 1.13, 1.76, 2.25 and 3.10 W/(m K), the outer surface of material presents a decreasing peak temperature of 163.2 °C, 102.7 °C, 91.7 °C, 86.7 °C, and 81.2 °C. This is due to the fact that increasing the thermal conductivity provides better heat dissipation. Especially it implies that the material with 0 wt% expanded graphite cannot be used, because its low thermal conductivity slows the heat transfer in the material. The results also indicated that the shape-stabilized PCM can effectively absorb the heat to prevent the thermal control system faults when the spacecraft's outer heat flux changes dramatically [77].

The shape-stabilized PCM was adopted for constructing heat storage condensers. A novel household refrigerator equipped with the heat storage condensers was setup based on an ordinary double-door compartment refrigerator. The results showed that the overall heat-transfer performances of the refrigerator can be significantly improved by addition of the shape-stabilized PCM as heat storage material, which allowed continuous heat dissipation for the condensers during a complete cycle. The condenser midpoint temperature was decreased by 2.3 °C and the condenser outlet temperature was decreased by 6.5 °C, which was only higher than the ambient temperature (25.5 °C) by 0.5 °C. This result indicated that a lower condensation temperature and a larger subcooling degree at the condenser outlet were achieved. Thus, the efficiency of the cooling system could be greatly improved. Under the test conditions, the energy consumptions of the novel and the ordinary refrigerators were 0.45 kWh and 0.51 kWh, respectively, which indicated that the novel refrigerator can save energy by 12% [78].

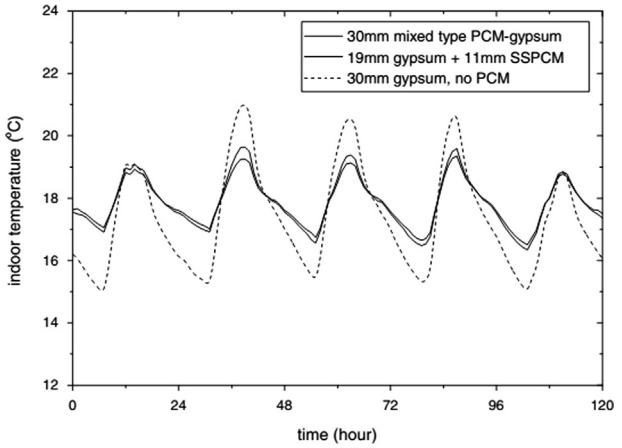


Fig. 16. Indoor temperature variation with the two types of PCM composites [76].

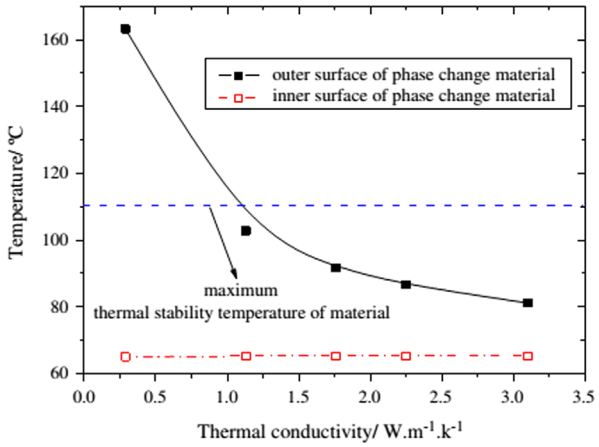


Fig. 17. The effect of thermal conductivity on the thermal control of spacecraft [77].

Some applications of the shape-stabilized PCM in energy efficient buildings were studied and validated by the experiments. The results showed that the optimal composition of the paraffin in shape-stabilized PCM is about 80%, and its fusion latent heat is in the range of 120–160 kJ/kg. It is found that for PCM floor or wallboard to absorb solar energy to narrow the temperature swing in a day in winter, the suitable melting temperature of the PCM is 2 °C higher than the average indoor air temperature of the room without PCM for the period of sunshine. For the electric under-floor space heating system, the optimal melting temperature is about 40 °C. The PCM layer used in the application should not be thicker than 2 cm [79].

The PCMs incorporated in building structures can increase their thermal inertia without increasing their volume. A polymer composite PCM containing 85% of paraffin, with a melting latent heat of 110 kJ/kg and a melting point of 27 °C, was incorporated in a hollow concrete floor panel. The experimental results showed that the influence of PCM, namely a decrease of the surface wall temperature amplitude and an increase of thermal energy stored. A numerical simulation confirmed the enhancement of the floor inertia by the incorporation of the PCM. The simulation provided design guidelines for the thermal management system to minimize the quantity and size of the PCM [80].

The PCM incorporated in panels can achieve important energy savings in buildings and maintain the indoor thermal comfort. Therefore, the PCM panels encapsulating capric acid (CA) were installed on the outside surface in one room and the PCM panels encapsulating the mixture of the CA and 1-dodecanol (CADE) with a melting point of 26.5 °C were used inside building. Three operation measures, inclusive of free cooling, open window and door at night and forced ventilation at night with a low-power air exhauster, were carried out in experimental process in summer. The results indicated that both the PCMOW (outer surface of walls and roofs) and PCMIW (inside surface of walls and roofs) rooms were about 1 °C and more than 2 °C cooler than the reference room, and the inside temperature peaks were lagged. The maximum temperature in the wall with PCM panels appeared about 2–3 h later than that of the wall without PCM. This result revealed that the thermal inertia of the PCMOW and PCMIW wall was higher. The thermal lag of 2–3 h indicated a large reduction in the electrical consumption from air conditioning [81].

5.2. Applications of microencapsulated phase change materials

Microencapsulated PCMs have been recognized as effective materials to enhance heat transfer, and to improve heat storage performance in thermal energy system. Microencapsulated PCM slurry can apply to heat transport and thermal energy storage systems. In order to fully develop the application of the microencapsulated PCM slurry in thermal energy system, more researches on applications and characteristics of the microencapsulated PCM slurry have been performed [82].

A successful way to enhance the thermal capacity of secondary fluid systems is by incorporating microencapsulated PCM slurry. The experimental results showed that the microencapsulated PCM slurry can provide considerable heat capacity in heat transfer applications. The microencapsulated PCM slurries exhibited a Newtonian-like behavior at mass fractions below 17.7%, and the relative viscosity is independent of temperature. Microcapsules become durable and impact-resistant when smaller than 10 μm. The heat transfer experiments indicated that the heat capacity enhancements are considerable even at low mass fractions. The heat transfer coefficient increases considerably during the phase change process [83].

A new type of functional fluid, magnetic microencapsulated phase change material (MMPCM) suspension, was proposed and prepared. The apparent specific heat capacity and thermal conductivity of MMPCM suspension were investigated. The apparent specific heat capacity of the MMPCM suspension greatly depends upon the fluid temperature and exquisitely changes among the three possible regions such as the solid-state, phase-change, and liquid-state. In the phase-change region, the apparent specific heat capacity of the suspension is larger than that in other two regions. The higher the volume fraction of the MMPCM particles is, the larger the peak value of apparent specific heat capacity of the suspension is. The thermal conductivity ratio increases linearly with the volume fraction of the MMPCM particles and also increases with increase in the content of iron nanoparticles inside the MMPCM particles. Iron nanoparticles can enhance the thermal conductivity of the suspension and make the particles magnetic. Among all components of the MMPCM particles, the content of iron nanoparticles is the dominating factor of affecting the thermal conductivity of the suspension [84].

The heat storage characteristics in the PCM microcapsule slurry were investigated in a horizontal rectangular enclosure constantly heated from the bottom. The experimental results indicated that the PCM in the slurry has a large effect on heat storage. It cannot only promote natural convection heat transfer but also lengthen the heat storage completion time due to the latent heat in the slurry. The results also revealed that the heat storage capacity increases with the mass concentration and the heat storage temperature, and the maximum local heat transfer coefficient increases with a decrease in mass concentration at the low heat temperature. It is found that an increase in mass concentration and height of the enclosure prolonged the completion time of heat storage in the PCM microcapsule slurry [85].

The microencapsulated PCM slurry (MEPCS) at high concentration (45% w/w) was developed based on microencapsulated Rubitherm RT6. Its heat storage and heat transfer characteristics were investigated in order to assess its suitability for integration into a low temperature heat storage system. It is found that inside the phase change interval the value of the heat transfer coefficient for the MEPCS was 5 times higher than for water under identical temperature conditions. For values of the bulk fluid temperature above 20 °C, the heat transfer coefficient for water became higher than for MEPCS. The significant correlation was identified between the value of the heat transfer coefficient for MEPCS and for water [86].

The experimental tests were performed at a set-up which consists of several cubicles where different construction materials may be tested for thermal energy storage purposes in a Mediterranean climate. The addition of microencapsulated PCM into two concrete made cubicles (with no insulation) had been previously tested with good results. However, due to the climatic conditions did not allow PCM to complete full phase change cycles during the summer, awnings were added to the cubicles. Free-cooling and open windows tests were carried out. It is found that the PCM effects were favored by the awnings, as peak temperature reductions were increased about 6%, their appearance delay was increased 36% (free-cooling), but decreased 14% (open windows), and the time in comfort conditions increased between 10% and 21%. The active hours of the PCM were increased 4–10% [87].

The heat transfer characteristics of the microencapsulated PCM (MPCM) suspension, formed by microencapsulating industrial-grade 1-bromohexadecane ($C_{16}H_{33}Br$) as PCM, were investigated for laminar flow in a circular tube under constant heat flux. The experimental results indicated that the dimensionless internal wall temperature of the MPCM suspension is lower than pure water, and the decrease can be up to 30% of that of water. It is found that the heat transfer enhancement ratio for 15.8 wt% MPCM suspension is 1.42 times higher than that for water. The results also showed that the pump consumption of the MPCM suspension system decreased greatly for the larger heat transfer

rate compared with water, and the decrease was up to 67.5% of that of water at *qs*750 W (15.8 wt%) [88].

The melting and freezing temperatures as well as the latent heat of the gypsum board with 50 wt% or 60 wt% microencapsulated PCMs (micro-PCMs) and 3 wt% glass fibers are quite suitable for the potential thermal energy storage of building applications. The gypsum boards with micro-PCMs showed a good thermal-regulated property. It is found that the temperature of the gypsum board incorporated with 60 wt% micro-PCMs can be kept in the range of 22–27 °C for about 1735 s due to the phase change of the inside micro-PCMs. The thermal-regulated gypsum boards also presented excellent thermal cycling stability, high thermal capacity and thermal conductivity, especially for the sample incorporated with 50 wt% micro-PCMs. The results indicated that the impregnation of the micro-PCMs into constructions can improve the thermal capacity and comfort of buildings [89].

A water based suspension containing microencapsulated phase change material (MEPCM) and multi-walled carbon nanotubes (MWCNT) was prepared as a heat transfer fluid. The experimental investigations were performed to study thermal and rheological properties of the blended fluids. It is found that the thermal conductivity of the blended fluids increases non-linearly with the MWCNT mass fraction, and a maximum increase of 8% in thermal conductivity was achieved for a 10 wt% MEPCM and 1 wt% MWCNT blend as compared to the pure MPCS. The results indicated that a 10 wt% MEPCM and 1 wt% MWCNT blend has an optimal thermal performance and stability and it has great potential as an improved heat transfer fluid [90].

The experimental investigation using microencapsulated PCM slurry with a 10% weight concentration of paraffin was performed as a thermal storage material and heat transfer fluid. The results demonstrated an improvement of approximately 25% on the convective heat transfer coefficient when compared to water. The experimental results showed that the microencapsulated PCM slurry can provide considerable advantages for thermal storage systems as well as heat transfer applications, and the energy stored in the phase change temperature range was 75% higher than the stored energy in the same temperature range with water. It is found that wall temperature for microencapsulated PCM slurry was lower than that for water due to the phase change process, and local convective heat transfer coefficient was approximately 25% higher than that for water [91].

5.3. Applications of shape-stabilized phase change materials in engineering project

5.3.1. Applications of composite phase change materials in engineering project

A new kind of under-floor electric heating system with shape-stabilized phase change material (PCM) plate was investigated by Lin et al. [92]. The experimental house with 3 m (depth) × 2 m (width) × 2 m (height) was built, as shown in Fig. 18. The apparatus ran for 6 days with night electric heating, and then for 4 days without electric heating. During the experiment, the heaters stopped working when their temperature is higher than 70 °C and operated again when it is smaller than 55 °C in the heating period from 23:00 to 8:00. The results showed that the average indoor temperature was 20 °C and the temperature difference between day and night was 12 °C without electric heating, and the average indoor temperature was 31 °C and the temperature difference between day and night was still kept around 12 °C with night electric heating. It is found that the temperature of the PCM plate's upper surface was kept above 45 °C for more than 10 h after heaters stopped working at 8:00, and the temperature difference between the two indoor measuring points (0.5 and 1.5 m high) was less than 0.5 °C. Therefore, the heating system was comfortable and energy-efficient.



Fig. 18. The experimental house with 3 m (depth) × 2 m (width) × 2 m (height) [92].

In order to acquire the thermal performances of the under-floor electric heating system with ductless air supply and the shape-stabilized PCM plates, an experimental house with this system was established by Lin et al. at Tsinghua University, China [93]. Fig. 19 shows the schematic diagram of the heating system and the wall. The under-floor heating system consists of 120-mm thick polystyrene insulation, electric heaters, 15-mm-thick PCM, 50-mm-thick air layer, 40-mm-thick floor cover material, cylindrical supporters, air inlets and air outlets with fans. The electrical heating system worked for five days with ductless air supply and then for 5 days without air supply. The test program is as follows for the first 5 days: the electrical heaters ran during the off-peak period 23:00–7:00, while they stopped working when their temperatures were higher than 65 °C or during period 7:00–23:00. The test results showed that the average indoor peak temperature was increased by 8 °C with ductless air supply, while the temperature at night was maintained low. The PCM surface temperature was higher than 45 °C all the time. It is observed that the temperature difference was less than 0.5 °C without air supply and less than 1.0 °C with air supply. This project demonstrated the total electrical energy consumption could be changed from the peak period to the off-peak period, which would bring significant economic benefits due to the different electricity tariff between day and night.

In order to test the thermal storage performances of the composite thermal storage gypsum boards, the gypsum boards of the RT20/montmorillonite composite PCM were fabricated by Fang and Zhang [94]. Five pieces of ordinary gypsum boards and a top board were used to build a small test room (70 mm × 70 mm × 70 mm). Three test rooms were constituted with different top boards: one is an ordinary gypsum board, the others are two composite gypsum boards with 20% and 50% of the RT20/montmorillonite composite. The test results presented that the maximum difference in the outside wall temperature of the top board between the indoor temperature of the test room was 10.5 °C for the test room with an ordinary gypsum board as the top board, 16.5 °C for the test room with the composite gypsum board with 20% of the RT20/montmorillonite composite PCM as the top board, and 20.0 °C for the composite gypsum board with 50% of the RT20/montmorillonite composite PCM. It is known that the maximum indoor temperature of the three test rooms was 40 °C for the ordinary gypsum board as the top board, 35 °C and 31 °C for the composite gypsum boards with 20% and 50% of the

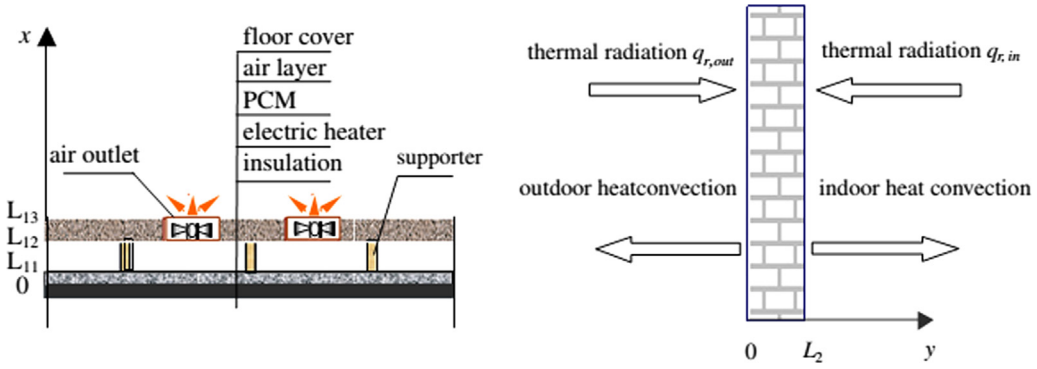


Fig. 19. Schematic diagram of the heating system and the wall [93].



Fig. 20. Temperature measurement on the surfaces of the tiles with PCM and without PCM [96].

RT20/montmorillonite composite, respectively. These results indicated that the composite gypsum boards could improve human comfort by reducing the indoor temperature swings and maintaining the temperature closer to the desired temperature.

The experimental tests were conducted to investigate the thermal performance of the tile with PCM and thermal insulation on the floor [95]. The temperatures were measured continuously on the surfaces of the tiles with PCM and without PCM, as shown in Fig. 20. The test results showed that the increase of the temperature at the surface of the tile with PCM reached values between 1.5 °C and 2.0 °C over the temperature at the surface of the tile without PCM. It is observed that the tiles with PCM could regulate surface temperature to an average between 4 °C and 10 °C with regard to conventional tiles without PCM. This project demonstrated that the average thermal discharge time of the tile with PCM placed over thermal insulation is 20 h, making it coincide with the beginning of a new period of solar radiation.

5.3.2. Applications of microencapsulated phase change materials in engineering project

The innovative concrete with phase change materials was developed to achieve important energy savings in buildings. The construction and experimental installation of two real size concrete cubicles to investigate the effect of the inclusion of a phase change material with a melting point of 26 °C, and a phase change enthalpy of 110 kJ/kg were carried out by Cabeza et al. [96]. The experimental results showed that the cubicle without PCM has a maximum temperature 1 °C higher than that with phase change material, and a minimum temperature 2 °C lower. It is found that the maximum temperature in the wall with phase change material takes place about 2 h later without PCM, and this thermal inertia appears again in the afternoon due to the freezing of the PCM, but also earlier in the morning due to the melting of the phase change material. These results indicated that the energy storage in the walls by encapsulating PCMs can lead to an improved thermal inertia as well as lower inner temperatures. This project demonstrated a real investigation in energy savings for buildings.

The effect of positions (externally bonded, laminated within and internally bonded) of macro encapsulated PCM in concrete walls on indoor temperatures and humidity levels of room models was investigated by Shi et al. [97]. The experimental results showed that the model with PCM laminated within the concrete walls had the best temperature control and was effective in reducing the maximum temperature by up to 4 °C. However, the model with PCM placed on the inner side of concrete walls presented the best humidity control and reduced the relative humidity by 16% more than the control model. It is found that the variation in temperature difference in the control model and the ambient temperature is small with the maximum variation of 1.3 °C. However, the indoor temperature difference for the model with PCM was 2.1–4.4 °C lower than the control model. Therefore, it can be summarized that PCM shows better performance when the temperature difference between the day and night is large.

6. Conclusions and outlook

The preparation, thermal properties and applications of shape-stabilized thermal energy storage materials were summarized. The thermal characteristics of the composite phase change material and microencapsulated phase change material were described. The applications of shape-stabilized thermal energy storage materials were presented. The following conclusions and outlook can be drawn:

(1) The composite PCMs can be prepared by integrating the PCMs into inorganic and organic supporting materials. The leakage of the melted PCM during the phase change process can be avoided. The composite PCMs have high latent heat storage capacity and proper phase change temperatures for practical latent heat storage applications.
(2) The shape-stabilized PCMs can be prepared by microencapsulating the PCMs into the organic and inorganic shells. Microencapsulated PCMs can be achieved by physical method such as spray-drying and chemical method such as complex coacervation, interfacial polycondensation and in-situ polymerization. The microencapsulated PCMs can greatly increase the heat transfer efficient, and increase surface-to-volume ratio of phase change material. The shell of microcapsules can reduce

PCM reactivity towards the outside environment and controls the volume changes as phase change occurs.

(3) The applications of shape-stabilized thermal energy storage materials in building energy conservation have been developed. The shape-stabilized PCMs in building products can store significant amounts of thermal energy without large structural mass associated with sensible heat storage. It not only can reduce building energy consumption, but also flatten the fluctuation of indoor temperature and improve the indoor thermal environment and building performances.

(4) Microencapsulated PCMs have been recognized as effective materials to enhance heat transfer, and to improve heat storage performance in thermal energy system. Microencapsulated PCM slurry can apply to heat transport and thermal energy storage systems, and it can reduce the equipment size and power consumption of the pump. In addition to the increase in effective specific heat because of the latent heat of melting, the use of a PCM can also maintain a large temperature difference with the suspension temperature.

(5) In order to prevent leakage of the melted PCMs during the phase change process, various encapsulation techniques have been used to microencapsulate the PCMs. However, the preparation investigation on the microencapsulated PCMs is still in experimental phase because some problems must be solved, such as production rate of the microcapsules, cracking rate of the shells, the thermal stability and durability of the microcapsules, compatibility with materials, cost of preparation, etc.

The future directions for PCM research are focused on following aspects: (a) the new-style solid–solid composite PCMs should be developed to prevent leakage of the melted PCMs, (b) in order to improve heat transfer rate of the composite PCMs, the higher thermal conductivity composite PCMs need to be investigated, and (c) besides building applications for thermal energy storage and air-conditioning systems for cooling and heating storage, the shape-stabilized PCMs will be investigated in textile applications to improve the thermo-regulating efficiency of fabrics, electronic equipment thermal management systems to control the operating temperature of electronic modules, photovoltaic-thermal modules to store thermal energy and control the temperature of photovoltaic-thermal modules, and aerospace equipment applications as thermal controlling materials.

Acknowledgments

This project is supported by the National Natural Science Foundation of China (Grant no. 51376087) and the Priority Academic Program Development of Jiangsu Higher Education Institutions. The authors also wish to thank reviewers for kindly giving revising suggestions.

References

[1] Agyenim F, Hewitt N, Eames P, Smyth M. A review of materials, heat transfer and phase change problem formulation for latent heat thermal energy storage systems (LHTESS). Renew Sustain Energy Rev 2010;14:615–28.
[2] Felix RA, Solanki SC, Saini JS. Heat transfer characteristics of thermal energy storage system using PCM capsules: a review. Renew Sustain Energy Rev 2008;12:2438–58.
[3] Shukla A, Buddhi D, Sawhney RL. Solar water heaters with phase change material thermal energy storage medium: a review. Renew Sustain Energy Rev 2009;13:2119–25.
[4] Hasnain SM. Review on sustainable thermal energy storage technology, part II: cool thermal storage. Energy Convers Manag 1998;39:1139–53.
[5] Kenisarin M, Mahkamov K. Solar energy storage using phase change materials. Renew Sustain Energy Rev 2007;11:1913–65.
[6] Tuncbilek K, Sari A, Tarhan S, Ergunes G, Kaygusuz K. Lauric and palmitic acids eutectic mixture as latent heat storage material for low temperature heating applications. Energy 2005;30:677–92.
[7] Alkan C, Sari A. Fatty acid/poly(methyl methacrylate) (PMMA) blends as form-stable phase change materials for latent heat thermal energy storage. Solar Energy 2008;82:118–24.
[8] Chen CZ, Wang LG, Huang Y. A novel shape-stabilized PCM: electrospun ultrafine fibers based on lauric acid/polyethylene terephthalate composite. Mater Lett 2008;62:3515–7.
[9] Cai YB, Hu Y, Song L, Lu HD, Chen ZY, Fan WC. Preparation and characterizations of HDPE–EVA alloy/OMT nanocomposites/paraffin compounds as a shape stabilized phase change thermal energy storage material. Thermochim Acta 2006;451:44–51.
[10] Tian T, Song J, Niu LB, Feng RX. Preparation and properties of 1-tetradecanol/1,3:2,4-di-(3,4-dimethyl) benzylidene sorbitol gelatinous form-stable phase change materials. Thermochim Acta 2013;554:54–8.
[11] Senturk SB, Kahraman D, Alkan C, Gokce I. Biodegradable PEG/cellulose, PEG/agarose and PEG/chitosan blends as shape stabilized phase change materials for latent heat energy storage. Carbohydr Polym 2011;84:141–4.
[12] Sari A. Form-stable paraffin/high density polyethylene composites as solid–liquid phase change material for thermal energy storage: preparation and thermal properties. Energy Convers Manag 2004;45:2033–42.
[13] Cai YB, Ke HZ, Lin L, Fei XZ, Wei QF, Song L, et al. Preparation, morphology and thermal properties of electrospun fatty acid eutectics/polyethylene terephthalate form-stable phase change ultrafine composite fibers for thermal energy storage. Energy Convers Manag 2012;64:245–55.
[14] Wang LJ, Meng D. Fatty acid eutectic/polymethyl methacrylate composite as form-stable phase change material for thermal energy storage. Appl Energy 2010;87:2660–5.
[15] Qian Y, Wei P, Jiang PK, Li Z, Yan YG, Liu JP. Preparation of a novel PEG composite with halogen-free flame retardant supporting matrix for thermal energy storage application. Appl Energy 2013;106:321–7.
[16] Memon SA, Lo TY, Barbhuiya SA, Xu WT. Development of form-stable composite phase change material by incorporation of dodecyl alcohol into ground granulated blast furnace slag. Energy Build 2013;62:360–7.
[17] Chen CZ, Wang LG, Huang Y. Morphology and thermal properties of electrospun fatty acids/polyethylene terephthalate composite fibers as novel form-stable phase change materials. Sol Energy Mater Sol Cells 2008;92:1382–7.
[18] Cheng WL, Zhang RM, Xie K, Liu N, Wang J. Heat conduction enhanced shape-stabilized paraffin/HDPE composite PCMs by graphite addition: preparation and thermal properties. Sol Energy Mater Sol Cells 2010;94:1636–42.
[19] Mei DD, Zhang B, Liu RC, Zhang YT, Liu JD. Preparation of capric acid/halloysite nanotube composite as form-stable phase change material for thermal energy storage. Sol Energy Mater Sol Cells 2011;95:2772–7.
[20] Cai YB, Zong X, Zhang JJ, Hu YY, Wei QF, He GF, et al. Electrospun nanofibrous mats absorbed with fatty acid eutectics as an innovative type of form-stable phase change materials for storage and retrieval of thermal energy. Sol Energy Mater Sol Cells 2013;109:160–8.
[21] Zeng JL, Zhu FR, Yu SB, Xiao ZL, Yan WP, Zheng SH, et al. Myristic acid/polyaniline composites as form stable phase change materials for thermal energy storage. Sol Energy Mater Sol Cells 2013;114:136–40.
[22] Cheng WL, Liu N, Wu WF. Studies on thermal properties and thermal control effectiveness of a new shape-stabilized phase change material with high thermal conductivity. Appl Therm Eng 2012;36:345–52.
[23] Karaipekli A, Sari A. Capric–myristic acid/vermiculite composite as form-stable phase change material for thermal energy storage. Sol Energy 2009;83:323–32.
[24] Mehrali M, Latibari ST, Mehrali M, Metselaar HSC, Silakhori M. Shape-stabilized phase change materials with high thermal conductivity based on paraffin/graphene oxide composite. Energy Convers Manag 2013;67:275–82.
[25] Bicer A, Sari A. New kinds of energy-storing building composite PCMs for thermal energy storage. Energy Convers Manag 2013;69:148–56.
[26] Li M, Wu ZS, Tan JM. Properties of form-stable paraffin/silicon dioxide/expanded graphite phase change composites prepared by sol–gel method. Appl Energy 2012;92:456–61.
[27] Fang GY, Li H, Liu X. Preparation and properties of lauric acid/silicon dioxide composites as form-stable phase change materials for thermal energy storage. Mater Chem Phys 2010;122:533–6.
[28] Wang WL, Yang XX, Fang YT, Ding J. Preparation and performance of form-stable polyethylene glycol/silicon dioxide composites as solid–liquid phase change materials. Appl Energy 2009;86:170–4.
[29] Fang GY, Li H, Chen Z, Liu X. Preparation and characterization of flame retardant n-hexadecane/silicon dioxide composites as thermal energy storage materials. J Hazard Mater 2010;181:1004–9.
[30] Li M, Wu ZS, Kao HT. Study on preparation, structure and thermal energy storage property of capric–palmitic acid/attapulgite composite phase change materials. Appl Energy 2011;88:3125–32.
[31] Fang GY, Li H, Chen Z, Liu X. Prep aration and characterization of stearic acid/expanded graphite composites as thermal energy storage materials. Energy 2010;35:4622–6.
[32] Mehrali M, Latibari ST, Mehrali M, Mahlia TMI, Metselaar HSC. Preparation and properties of highly conductive palmitic acid/graphene oxide composites as thermal energy storage materials. Energy 2013;58:628–34.

[33] Fang GY, Li H, Cao L, Shan F. Preparation and thermal properties of form-stable palmitic acid/active aluminum oxide composites as phase change materials for latent heat storage. Mater Chem Phys 2012;137:558–64.
[34] Karaipekli A, Sari A. Preparation and characterization of fatty acid ester/building material composites for thermal energy storage in buildings. Energy Build 2011;43:1952–9.
[35] Sari A, Karaipekli A. Preparation, thermal properties and thermal reliability of palmitic acid/expanded graphite composite as form-stable PCM for thermal energy storage. Sol Energy Mater Sol Cells 2009;93:571–6.
[36] Chen Z, Shan F, Cao L, Fang GY. Preparation and thermal properties of n-octadecane/molecular sieve composites as form-stable thermal energy storage materials for buildings. Energy Build 2012;49:423–8.
[37] Karaman S, Karaipekli A, Sari A, Bicer A. Polyethylene glycol (PEG)/diatomite composite as a novel form-stable phase change material for thermal energy storage. Sol Energy Mater Sol Cells 2011;95:1647–53.
[38] Fang GY, Li H, Chen Z, Liu X. Preparation and properties of palmitic acid/SiO_2 composites with flame retardant as thermal energy storage materials. Sol Energy Mater Sol Cells 2011;95:1875–81.
[39] Karaipekli A, Sari A. Capric–myristic acid/expanded perlite composite as form-stable phase change material for latent heat thermal energy storage. Renew Energy 2008;33:2599–605.
[40] Li H, Liu X, Fang GY. Preparation and characteristics of n-nonadecane/cement composites as thermal energy storage materials in buildings. Energy Build 2010;42:1661–5.
[41] Li BX, Liu TX, Hu LY, Wang YF, Nie SB. Facile preparation and adjustable thermal property of stearic acid–grapheme oxide composite as shape-stabilized phase change material. Chem Eng J 2013;215–216:819–26.
[42] Chen Z, Shan F, Cao L, Fang GY. Synthesis and thermal properties of shape-stabilized lauric acid/activated carbon composites as phase change materials for thermal energy storage. Sol Energy Mater Sol Cells 2012;102:131–6.
[43] Sari A, Alkan C, Karaipekli A, Uzun O. Microencapsulated n-octacosane as phase change material for thermal energy storage. Sol Energy 2009;83:1757–63.
[44] Ma YH, Chu XD, Tang GY, Yao YW. The effect of different soft segments on the formation and properties of binary core microencapsulated phase change materials with polyurea/polyurethane double shell. J Colloid Interface Sci 2013;392:407–14.
[45] Qiu XL, Song GL, Chu XD, Li XZ, Tang GY. Microencapsulated n-alkane with p(n-butyl methacrylate-co-methacrylic acid) shell as phase change materials for thermal energy storage. Sol Energy 2013;91:212–20.
[46] Fang GY, Li H, Liu X, Wu SM. Experimental investigation of performances of microcapsule phase change material for thermal energy storage. Chem Eng Technol 2010;33:227–30.
[47] Qiu XL, Song GL, Chu XD, Li XZ, Tang GY. Preparation, thermal properties and thermal reliabilities of microencapsulated n-octadecane with acrylic-based polymer shells for thermal energy storage. Thermochim Acta 2013;551:136–44.
[48] Fuensanta M, Paiphansiri U, Romero-Sanchez MD, Guillem C, Lopez-Buendia AM, Landfester K. Thermal properties of a novel nanoencapsulated phase change material for thermal energy storage. Thermochim Acta 2013;565:95–101.
[49] Chen L, Xu LL, Shang HB, Zhang ZB. Microencapsulation of butyl stearate as a phase change material by interfacial polycondensation in a polyurea system. Energy Convers Manag 2009;50:723–9.
[50] Alkan C, Sari A, Karaipekli A. Preparation, thermal properties and thermal reliability of microencapsulated n-eicosane as novel phase change material for thermal energy storage. Energy Convers Manag 2011;52:687–92.
[51] Zhang T, Wang Y, Shi H, Yang WT. Fabrication and performances of new kind microencapsulated phase change material based on stearic acid core and polycarbonate shell. Energy Convers Manag 2012;64:1–7.
[52] Sari A, Alkan C, Karaipekli A. Preparation, characterization and thermal properties of PMMA/n-heptadecane microcapsules as novel solid–liquid microPCM for thermal energy storage. Appl Energy 2010;87:1529–34.
[53] Qiu XL, Li W, Song GL, Chu XD, Tang GY. Microencapsulated n-octadecane with different methylmethacrylate-based copolymer shells as phase change materials for thermal energy storage. Energy 2012;46:188–99.
[54] Alkan C, Sari A, Karaipekli A, Uzun O. Preparation, characterization, and thermal properties of microencapsulated phase change material for thermal energy storage. Sol Energy Mater Sol Cells 2009;93:143–7.
[55] Fang GY, Li H, Yang F, Liu X, Wu SM. Preparation and characterization of nano-encapsulated n-tetradecane as phase change material for thermal energy storage. Chem Eng J 2009;153:217–21.
[56] Huang J, Wang TY, Zhu PP, Xiao JB. Preparation, characterization, and thermal properties of the microencapsulation of a hydrated salt as phase change energy storage materials. Thermochim Acta 2013;557:1–6.
[57] Zhang HZ, Wang XD, Wu DZ. Silica encapsulation of n-octadecane via sol–gel process: a novel microencapsulated phase-change material with enhanced thermal conductivity and performance. J Colloid Interface Sci 2010;343:246–55.
[58] Chen Z, Cao L, Shan F, Fang GY. Preparation and characteristics of micro-encapsulated stearic acid as composite thermal energy storage material in buildings. Energy Build 2013;62:469–74.
[59] Pan L, Tao QH, Zhang SD, Wang SS, Zhang J, Wang SH, et al. Preparation, characterization and thermal properties of micro-encapsulated phase change materials. Sol Energy Mater Sol Cells 2012;98:66–70.
[60] Zhang HZ, Sun SY, Wang XD, Wu DZ. Fabrication of microencapsulated phase change materials based on n-octadecane core and silica shell through interfacial polycondensation. Colloids Surf A: Physicochem Eng Asp 2011;389:104–17.
[61] Fang GY, Chen Z, Li H. Synthesis and properties of microencapsulated paraffin composites with SiO_2 shell as thermal energy storage materials. Chem Eng J 2010;163:154–9.
[62] Ma YH, Chu XD, Li W, Tang GY. Preparation and characterization of poly(methyl methacrylate-co-divinylbenzene) microcapsules containing phase change temperature adjustable binary core materials. Sol Energy 2012;86:2056–66.
[63] Su JF, Wang XY, Wang SB, Zhao YH, Huang Z. Fabrication and properties of microencapsulated-paraffin/gypsum-matrix building materials for thermal energy storage. Energy Convers Manag 2012;55:101–7.
[64] Zhang HZ, Wang XD. Fabrication and performances of microencapsulated phase change materials based on n-octadecane core and resorcinol-modified melamine–formaldehyde shell. Colloids Surf A: Physicochem Eng Asp 2009;332:129–38.
[65] Salaun F, Devaux E, Bourbigot S, Rumeau P. Influence of process parameters on microcapsules loaded with n-hexadecane prepared by in situ polymerization. Chem Eng J 2009;155:457–65.
[66] Cho JS, Kwon A, Cho CG. Microencapsulation of octadecane as a phase change material by interfacial polymerization in an emulsion system. Colloid Polym Sci 2002;280:260–6.
[67] Sanchez-Silva L, Rodriguez JF, Romero A, Borreguero AM, Carmona M, Sanche P. Microencapsulation of PCMs with a styrene-methyl methacrylate copolymer shell by suspension-like polymerization. Chem Eng J 2010;157:216–22.
[68] Qiu XL, Li W, Song GL, Chu XD, Tang GY. Fabrication and characterization of microencapsulated n-octadecane with different crosslinked methylmethacrylate-based polymer shells. Sol Energy Mater Sol Cells 2012;98:283–93.
[69] Tahan Latibari S, Mehrali M, Mehrali M, Indra Mahlia TM, Cornelis Metselaar HS. Synthesis, characterization and thermal properties of nanoencapsulated phase change materials via the sol–gel method. Energy 2013;61:664–72.
[70] Cao L, Tang F, Fang GY. Synthesis and characterization of microencapsulated paraffin with titanium dioxide shell as shape-stabilized thermal energy storage materials in buildings. Energy Build 2014;72:31–7.
[71] Konuklu Y, Unal M, Paksoy HO. Microencapsulation of caprylic acid with different wall materials as phase change material for thermal energy storage. Sol Energy Mater Sol Cells 2014;120:536–42.
[72] Ozonur Y, Mazman M, Paksoy HO, Evliya H. Microencapsulation of coco fatty acid mixture for thermal energy storage with phase change material. Int J Energy Res 2006;30:741–9.
[73] Borreguero AM, Valverde JL, Rodriguez JF, Barber AH, Cubillo JJ, Carmona M. Synthesis and characterization of microcapsules containing Rubitherm RT27 obtained by spray drying. Chem Eng J 2011;166:384–90.
[74] Zhou GB, Yang YP, Xu H. Energy performance of a hybrid space-cooling system in an office building using SSPCM thermal storage and night ventilation. Sol Energy 2011;85:477–85.
[75] Yan QY, Huo R, Li LS. Experimental study on the thermal properties of the phase change material wall formed by different methods. Sol Energy 2012;86:3099–102.
[76] Zhou GB, Zhang YP, Wang X, Lin KP, Xiao W. An assessment of mixed type PCM–gypsum and shape-stabilized PCM plates in a building for passive solar heating. Sol Energy 2007;81:1351–60.
[77] Wu WF, Liu N, Cheng WL, Liu Y. Study on the effect of shape-stabilized phase change materials on spacecraft thermal control in extreme thermal environment. Energy Convers Manag 2013;69:174–80.
[78] Cheng WL, Mei BJ, Liu YN, Huang YH, Yuan XD. A novel household refrigerator with shape-stabilized PCM (phase change material) heat storage condensers: an experimental investigation. Energy 2011;36:5797–804.
[79] Zhang YP, Lin KP, Yang R, Di HF, Jiang Y. Preparation, thermal performance and application of shape-stabilized PCM in energy efficient buildings. Energy Build 2006;38:1262–9.
[80] Royon L, Karim L, Bontemps A. Thermal energy storage and release of a new component with PCM for integration in floors for thermal management of buildings. Energy Build 2013;63:29–35.
[81] Kong XF, Lu SL, Huang JY, Cai Z, Wei SS. Experimental research on the use of phase change materials in perforated brick rooms for cooling storage. Energy Build 2013;62:597–604.
[82] Chen Z, Fang GY. Preparation and heat transfer characteristics of microencapsulated phase change material slurry: a review. Renew Sustain Energy Rev 2011;15:4624–32.
[83] Alvarado JL, Marsh C, Sohn C, Phetteplace G, Newell T. Thermal performance of microencapsulated phase change material slurry in turbulent flow under constant heat flux. Int J Heat Mass Transf 2007;50:1938–52.
[84] Xuan YM, Huang Y, Li Q. Experimental investigation on thermal conductivity and specific heat capacity of magnetic microencapsulated phase change material suspension. Chem Phys Lett 2009;479:264–9.
[85] Zhang YL, Wang SF, Rao ZH, Xie JF. Experiment on heat storage characteristic of microencapsulated phase change material slurry. Sol Energy Mater Sol Cells 2011;95:2726–33.
[86] Diaconu BM, Varga S, Oliveira AC. Experimental study of natural convection heat transfer in a microencapsulated phase change material slurry. Energy 2010;35:2688–93.
[87] Arce P, Castellon C, Castell A, Cabeza LF. Use of microencapsulated PCM in buildings and the effect of adding awnings. Energy Build 2012;44:88–93.

[88] Chen BJ, Wang X, Zeng RL, Zhang YP, Wang XC, Niu JL, et al. An experimental study of convective heat transfer with microencapsulated phase change material suspension: laminar flow in a circular tube under constant heat flux. Exp Therm Fluid Sci 2008;32:1638–46.
[89] Zhang HZ, Xu QY, Zhao ZM, Zhang J, Sun YJ, Sun LX, et al. Preparation and thermal performance of gypsum boards incorporated with microencapsulated phase change materials for thermal regulation. Sol Energy Mater Sol Cells 2012;102:93–102.
[90] Zhang GH, Zhao CY. Thermal property investigation of aqueous suspensions of microencapsulated phase change material and carbon nanotubes as a novel heat transfer fluid. Renew Energy 2013;60:433–8.
[91] Delgado M, Lazaro A, Mazo J, Marin JM, Zalba B. Experimental analysis of a microencapsulated PCM slurry as thermal storage system and as heat transfer fluid in laminar flow. Appl Therm Eng 2012;36:370–7.
[92] Lin KP, Zhang YP, Xu X, Di HF, Yang R, Qin PH. Experimental study of under-floor electric heating system with shape-stabilized PCM plates. Energy Build 2005;37:215–20.
[93] Lin KP, Zhang YP, Di HF, Yang R. Study of an electrical heating system with ductless air supply and shape-stabilized PCM for thermal storage. Energy Convers Manag 2007;48:2016–24.
[94] Fang XM, Zhang ZG. A novel montmorillonite-based composite phase change material and its applications in thermal storage building materials. Energy Build 2006;38:377–80.
[95] Ceron I, Neila J, Khayet M. Experimental tile with phase change materials (PCM) for building use. Energy Build 2011;43:1869–74.
[96] Cabeza LF, Castellon C, Nogues M, Medrano M, Leppers R, Zubillaga O. Use of microencapsulated PCM in concrete walls for energy savings. Energy Build 2007;39:113–9.
[97] Shi X, Memonb SA, Tang WC, Cui HZ, Xing F. Experimental assessment of position of macro encapsulated phase change material in concrete walls on indoor temperatures and humidity levels. Energy Build 2014;71:80–7.